Applied Biochemistry and Biotechnology (2021) 193:2297–2330
https://doi.org/10.1007/s12010-021-03528-6

REVIEW ARTICLE

Fermentative molecular biohydrogen production from cheese whey: present prospects and future strategy

Raman Rao[1] · Nitai Basak[1]

Received: 11 November 2020 / Accepted: 8 February 2021/ Published online: 19 February 2021

Abstract

Waste-dependent fermentative routes for biohydrogen production present a possible scenario to produce hydrogen gas on a large scale in a sustainable way. Cheese whey contains a high portion of organic carbohydrate and other organic acids, which makes it a feasible substrate for biohydrogen production. In the present review, recent research progress related to fermentative technologies, which explore the potentiality of cheese whey for biohydrogen production as an effective tool on a large scale, has been analyzed systematically. In addition, application of multiple response surface methodology tools such as full factorial design, Box-Behnken model, and central composite design during fermentative biohydrogen production to study the interactive effects of different bioprocess variables for higher biohydrogen yield in batch, fed-batch, and continuous mode is also discussed. The current paper also emphasizes computational fluid dynamics–based simulation designs, by which the substrate conversion efficiency of the cheese whey–based bioprocess and temperature distribution toward the turbulent flow of reaction liquid can be enhanced. The possible future developments toward higher process efficiency are outlined.

Keywords Biohydrogen · Cheese whey · Dark fermentation · Photo fermentation · Optimization

Highlights
- Thorough discussion of metabolic pathway of lactic acid–producing bacteria for cheese whey fermentation and biochemistry of biohydrogen production from cheese whey by facultative anaerobes.
- Comprehensive summary of the state of the art of dark fermentation and sequential dark-photo fermentation to produce biohydrogen.
- Up-to-date consideration of response surface methodology to scale up biohydrogen production by optimizing process parameters.
- Holistic approach of computational fluid dynamics–based simulation to study hydrodynamic characteristics (gas-liquid flow) and temperature distribution inside the bioreactor configuration for synergistic improvement in biohydrogen production.

✉ Nitai Basak
basakn@nitj.ac.in; basakn812@yahoo.com

[1] Department of Biotechnology, Dr. B R Ambedkar National Institute of Technology, Jalandhar 144 011, India

Introduction

The extensive burning of non-conventional fuels is creating environmental problems and economic imbalance [1]. The uncontrolled burning of fossil fuel–based energy resources contributes to the emission of greenhouse gases, which is the leading cause of depletion of the ozone layer. Anthropogenic activities are responsible for 1°C increase in global warming globally, out of which 0.3°C increase is due to the burning of coal for electricity generation [2]. The rate of CO_2 emission due to industrial activities is increasing significantly with reported CO_2 level of 409 ppm in the atmosphere [3]. In this context, carbon capture technologies are of great significance and have the capability to mitigate CO_2 emissions from different sources. There are mainly three technologies that are crucial for carbon capturing and utilization: pre-combustion, post-combustion, and oxyfuel combustion [2]. Renewable sources of energy such as solar; wind; hydro- and biofuels like biodiesel, ethanol, and biogas; and biohydrogen ($bioH_2$) are given more focus across the world to develop future hydrogen (H_2) economy specially in terms of its use as fuel source. The $bioH_2$ is now worldwide accepted as an environmentally benign resource that has high energy density (143 GJ $tonne^{-1}$) and does not create greenhouse gas effect [4]. It releases only water vapor upon combustion. More focus has been given on $bioH_2$ production from renewable feedstocks, which are non-petroleum-based biomass. Renewable resource–based biological routes of H_2 production (Fig. 1) are less energy intensive and are environment friendly as compared to photo-electrochemical/thermochemical processes, which are energy intensive requiring energy in the form of heat or electricity to operate.

The biological methods can be broadly classified into (a) biofermentation (dark fermentation, DF, and photo fermentation, PF), (b) biophotolysis (direct and indirect method), (c) bioelectrochemical system such as microbial fuel cell (MFC), and (d) gasification method [3]. Out of the abovementioned methods, fermentative routes (Fig. 2) have been proven to be more helpful for developing future H_2 economy by utilizing methods involving photofermentative pathways [5] and/or anaerobic digestion process [6].

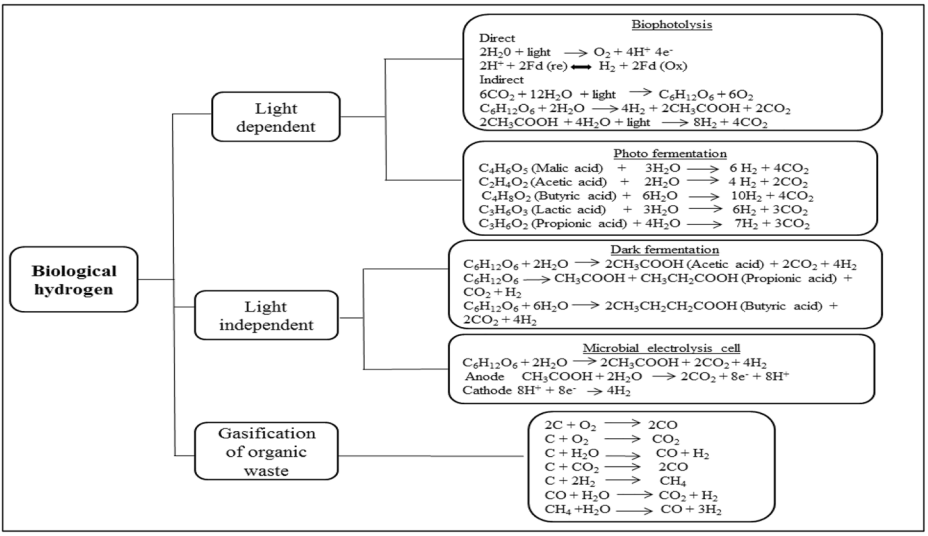

Fig. 1 Biological H_2 production methods

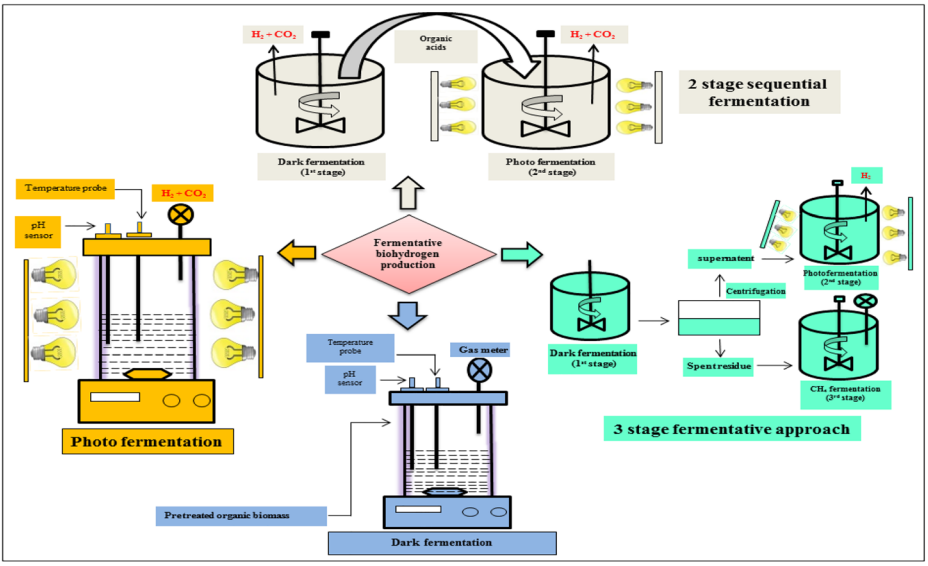

Fig. 2 Different strategies for fermentative H_2 production

DF process is a key promising biological method for the production of bioH_2 at a faster rate compared to biophotolysis from industrial organic wastewater by strict/facultative anaerobic bacteria [7, 8]. This approach provides dual benefits where negative valued wastewater can be utilized for renewable energy generation along with its treatment. The microbes grow on pure sugar as well as on organic feedstock through oxidations to increase their biomass and metabolic energy. However, only 30–40% of the energy stored in biomass is being converted into the bioH_2, and the rest of the 60–70% of biomass energy is converted into fermentative liquid waste (FLW) containing different metabolites like 1,3-propanediol, ethanol, acetic acid, and butyric acid [9]. Production of these by-products mainly depends upon the metabolic activity of H_2-producing bacteria [9]. The microbes convert glucose into pyruvate through glycolytic pathways producing adenosine triphosphate (ATP) from adenosine diphosphate (ADP) along with nicotinamide adenine dinucleotide (NADH) [10]. Pyruvate is then further oxidized to acetyl coenzyme A (acetyl-CoA), carbon dioxide (CO_2), and H_2 by pyruvate ferredoxin oxidoreductase (PFOR) and hydrogenase. Pyruvate may also be converted to acetyl-CoA and formate, which may further form H_2 and CO_2. In addition to formate, some other by-products such as acetate, butyrate, propionate, and ethanol may also be produced depending upon the operating conditions and type of H2-producing microbes [10]. PF has the following advantage: it produces biogas that is significantly pure and contains H_2 content equivalent to 80% [11]. Purple non-sulfur (PNS) microbial cell such as *Rhodobacter sphaeroides*, *Rhodobacter capsulatus*, and *Rhodopseudomonas palustris* are most suited for photofermentative H_2 production due to their efficient substrate degradation efficiency and them being able to utilize both visible and near-infrared regions of spectrum. The bacterium in the absence of oxygen assimilates organic acids such as malate and lactate (either in pure from or in waste water stream) into biomass, H_2, and CO_2 [12]. Further, dark fermentative biohydrogen production (DFBP) is likely to be feasible at an industrial level if integrated with another fermentation process, which can effectively utilize organic acids present in dark fermentative liquid waste [13]. Utilization of these acids toward effective photofermentative

H_2 generation is dependent upon operating conditions, viz. substrate concentration, temperature, pH, source of light, inoculum age of bacterial cell, and illumination intensity [14, 15]. The biological method of H_2 production using purple non-sulfur (PNS) bacteria during PF can utilize various feedstocks ranging from simple carbohydrates to complex polysaccharides. Photo fermenting microbes work efficiently at wide spectra of light energy having wavelength in the range of 500–900 nm [16]. The main enzyme that plays a role in H_2 production by photosynthetic bacteria is nitrogenase, whose activity is affected by presence of O_2 and NH_3 [17]. In addition, designing of a best possible configuration for photobioreactor (PBR) based on surface/volume ratio, growth conditions (temperature, pH, light source, light intensity, and its capability to penetrate inside the reactor), and light conversion efficiency (LCE) denoted by (η) is a prerequisite for attaining the good amount of photofermentative bioH_2 yield [18, 19]. LCE is calculated as per the following formula:

$$\text{LCE}\ (\%) = \frac{\text{Free energy of the total amount of hydrogen produced}}{\text{Total energy of incident light on reactor}} \times 100 \quad (1)$$

However, an efficient PBR with high light conversion efficiency is still considered as one of the important hurdles for enhancing the productivity and yield of bioH_2 at large scale.

In accordance with sustainable development and waste minimization issues, abundant organic wastewater from various industries such as dairy, sugarcane, and food processing could be the source for biohydrogen production using suitable bioprocess technologies where combination of waste treatment and energy production would be an advantage. The disposal of cheese whey (CW) directly into the environment severely affects the natural habitats, viz. depletion of dissolved oxygen reducing aquatic life and distorting the physical and chemical structure of soil [20]. Therefore, biotechnological remedial treatments have emerged as a permanent disposal method that can positively exploit the carbohydrate content of CW for the production of bioH_2 via fermentation route. CW is an ideal feedstock for fermentative bioH_2 production as it contains high organic concentration, mainly soluble carbohydrates [5]. The bioH_2 production by DF using CW requires facultative microorganisms because the presence of O_2 inhibits the working of the hydrogenase enzyme, which is crucial for producing bioH_2 [21]. The theoretical yield of bioH_2 in DF is 2 and 4 moles of H_2 mol^{-1} of glucose when end products are butyric acid and acetic acid, respectively [22]. Overall, CW-based DF process can be made cost-effective to scale up the process from lab scale to industrial level by maintaining optimum ratio of inoculum to substrate, by designing a cheap and long-lasting suitable bioreactor, studying the nature of inoculating microorganisms, performing a compositional analysis of CW, and knocking out of genes responsible for uptake hydrogenase with the help of genetic engineering tools. The presence of the high amount of carbohydrates (mainly lactose) and other volatile fatty acids (VFAs) in CW makes it a preferred substrate for bioH_2 production via anaerobic fermentation (either at a mesophilic or thermophilic range of temperature) being carried out by different bacterial cultures such as facultative microorganisms, viz. *Escherichia coli* and *Enterobacter* species, and some obligate anaerobic microbes, most importantly strains from *Clostridium* genus under mesophilic temperature (30–38°C) or thermophilic range of temperature [23, 24]. The biogas formed during the fermentation also contains CH_4 and CO_2. Additionally, during the anaerobic fermentation of CW, most of the energy of feedstock is utilized in forming the different organic acids [25], which in turn decreases the H_2 yield by lowering the pH of fermentation media. However, theoretically, complete conversion of electron equivalent in lactose to H_2 and CO_2 can produce up to 8 mol

of H_2 mol^{-1} lactose, which is still a significant challenge for the economical production of $bioH_2$ at industrial level [26]. Currently, bioprocessing of CW via integrated DF and PF is gaining prime interest with time as it has the capacity to produce $bioH_2$ with a yield equivalent to a theoretical yield of 12 mol of H_2 mol^{-1} glucose [27]. However, there are some challenges associated with the biological production of H_2 such as requirement of complicated treatment strategies for complex structure of organic biomass and availability of cheap feedstock. The comparative analysis of various biological routes of H_2 fermentation has proven water electrolysis to be the most promising route, in which the efficiency of electrolyzer has been reported in the range of 60–80%, whereas energy conversion efficiencies of DF, PF, biophotolysis cells, and microbial electrolysis cell are reported to be 4.3, 5.11, 4.0, and 11.3%, respectively [28, 29]. Very recently, an attempt was made by Sathyaprakashan and Kannan [30] to determine the overall cost of biological H_2 on the basis of substrate cost, inoculum cost, reactor layout, and operating cost (such as power, labor, water, general supply cost). The total operating cost of direct biophotolysis was highest (70,469 million USD) as compared to indirect biophotolysis (102.56 million USD), DF (981.53 million USD), and PF (193.69 million USD). Further, the cost for producing one kg of H_2 via direct biophotolysis, indirect biophotolysis, DF, and PF was 1342.27 million USD, 1.96 million USD, 18.70 million USD, and 3.70 million USD, respectively. However, production of H_2 by natural gas is the cheapest method reported so far around the globe, such as in Middle east region where production cost is one USD per one kg of H_2 [3]. Karthic and Joseph [31] compared the cost of biological routes of H_2 production with the cost associated in producing ethanol, gasoline, natural gas, and biodiesel. It was seen that hydrogen production using most of the available methods except pyrolysis was rather high in comparison to conventional methods of fuel production. Therefore, intensive R&D is required to make the biological H_2 production economically feasible. The cost for commercial production of $bioH_2$ can be reduced significantly by giving focus on two major factors: cost associated with the development of photobioreactor has to be brought down by using cheaper material for the fabrication of photobioreactors. Another important cost determining factor is the storage system required for a standalone system. Storage of H_2 in compressed form is useful for small quantities of gas, whereas the underground storage methods are beneficial for large volumes and for long-term storage. Cost reduction in this field would come only by the introduction of new or better technology.

From the literature review, it is clear that a review that solely highlights the anaerobic bioprocessing of CW by different fermentative strategies along with optimization of operational parameters and mathematical simulation of dark fermentative and photofermentative bioreactors leading to the high yield of $bioH_2$ is missing. Therefore, the main objective of this review paper is to bring the attention of all private and government entrepreneurs toward the potentiality of CW for producing $bioH_2$ so that the process can be taken to the industrial level to meet our daily energy demand without compromising with the need of our future generation. Moreover, the different metabolites produced during the fermentation of CW can be a potential source of various value-added products such as the substitute of phosphate-solubilizing biofertilizer [32], biobutanol [33], polyhydroxyalkanoates (PHAs) [34], and lipid [35]. As per the outcome of this present review, new technologies could be identified, which can be coupled with current research in the field of bioprocess engineering to develop a strategy to enhance the overall productivity of $bioH_2$.

CW characteristics

Cheese manufacturing industries generate yellow-colored liquid waste by-products, mainly CW, which has been proven as one of the economically feasible option for the production of bioH_2 via anaerobic fermentation leading to 8 mol of H_2 per mol of lactose as theoretical yield [24]. Every year globally, around 145 million tonnes of liquid CW is produced [36]. Out of this, about 58% is utilized for producing some value-added products such as cheese whey powder (CWP, which constituted around 50 million tonnes) and whey proteins (30 million tonnes), and around 5 million tonnes of CW is used to produce demineralized blends. The leftover 42% of CW is either discarded as effluent or is used for animal feeding. In recent years, many bioprocess techniques have come into the picture for the effective utilization of this vast amount of leftover CW for producing industry-oriented products (especially bioH_2).

Among the sugars, lactose is present in various by-products of dairy industries in addition to proteins, lipids, and mineral salts (NaCl, KCl, and calcium salts). Around 55% of the original milk nutrients [37, 38] and 80% contents of the original fermentation medium [39] constitute the CW. On an average, it contains (in w/v) 4.6% lactose, 1.2% crude protein, 0.3% fat, 5–8% total solids, 0.6% ash, and 92.7% water [40]. Biological oxygen demand (BOD) to chemical oxygen demand (COD) ratio of greater than 0.5 makes it a suitable feedstock for biotechnological treatment [41]. In addition to the abovementioned components, CW also contains some amount of citric acid, vitamin B, urea/uric acid, immunoglobulins, β-lactoglobulin, serum albumin, and α-lactoglobulin [42].

Biochemistry of lactic acid–producing bacteria for the fermentation of CW

A wide range of lactic acid bacteria (*Lactobacillus casei*, *Lactobacillus salivarius*, *Lactobacillus acidophilus*, and *Streptococcus* species) are known to produce lactic acid by fermenting the lactose present in CW. It has been estimated that around 72,000 tonnes of lactic acid (about 90% of the total production of lactic acid globally every year) is being produced by lactic acid bacteria alone [43]. Lactic acid–producing bacterial cells generally have two different types of metabolism for the fermentation of hexose/pentose sugar, viz. homolactic fermentative bacterial strains, which ferment five carbon sugars via pentose phosphate pathway and give a theoretical yield of 1.67 mol mol^{-1} pentose and six carbon sugars via the Embden-Meyerhof-Parnas (EMP) pathway producing 2 ATP molecules per molecule of glucose and 2 molecules of lactate per mol of glucose (theoretical yield of 2 mol mol^{-1} glucose) under optimum fermentation conditions [44] (Fig. 3).

Another pathway is heterolactic fermentation, in which hexose is metabolized via the EMP pathway producing lactic acid along with other by-products (ethanol, acetic acid, CO_2), respectively [45]. During heterolactic fermentation, *Lactobacillus* bacterial strain metabolizes five carbon sugar molecules such as xylose, arabinose, and ribose to first xylose 5-phosphate as an intermediate, which further breaks down to form glyceraldehyde-3-PO_4 and acetyl-P via phosphoketolase/phosphor gluconate (6 PG/PK)–dependent mechanism. The GAP is further metabolized to produce pyruvic acid followed by its final conversion to three carbon lactic acid and produce a theoretical lactic acid yield of 1 mol mol^{-1} sugar, whereas the acetyl-P further synthesizes other by-products such as ethanol and acetic acid [46]. The metabolism of different pentose sugars in case of facultative heterolactic bacterial strain may or may not result in the

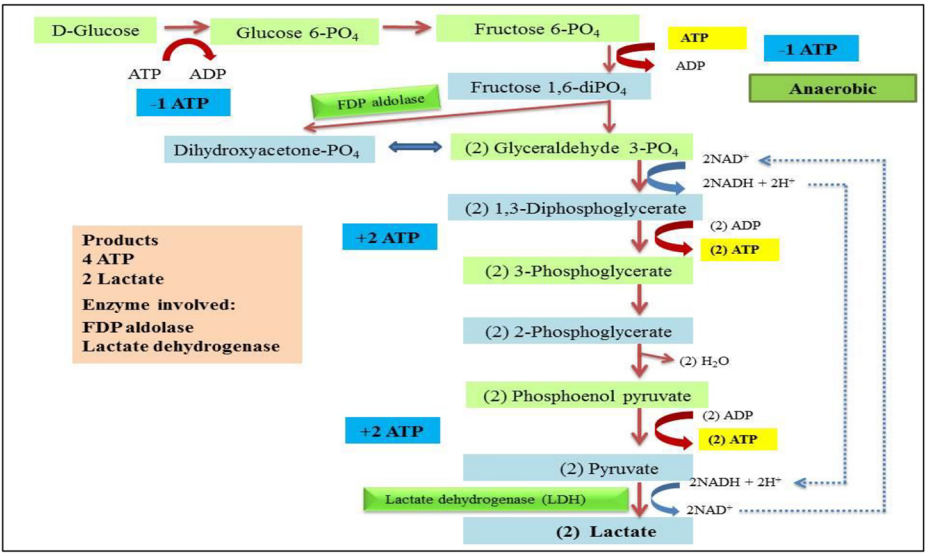

Fig. 3 Homolactic mode of fermentation

production of by-products depending upon the type of microbe chosen as the enzymes required for both the abovementioned pathways are present in these microbes [47]. Figure 4 depicts the biochemical pathway to produce lactate via heterolactic mode of fermentation.

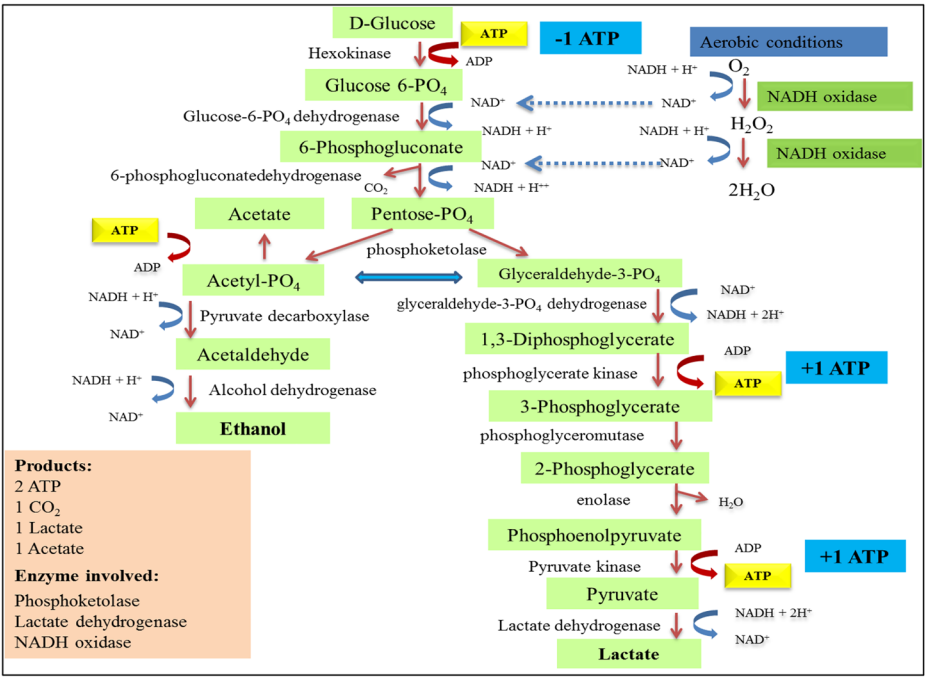

Fig. 4 Heterolactic mode of fermentation

Biochemistry for bioH_2 production by facultative anaerobes during DF of CW

As shown in Fig. 3, during glycolysis, two molecules of pyruvate are formed from a single molecule of glucose; therefore, maximum theoretical yield, which can be achieved, is 2 moles of H_2 mol^{-1} glucose. An enzyme complex, pyruvate formate lyase (PFL) to produce acetyl-CoA and formate, acts upon pyruvate formed during glycolysis. Facultative anaerobes such as *Enterobacter cloacae* IIT-BT08, *Enterobacter aerogenes*, and *Rhodospirillum rubrum* mediate H_2 production by breaking down the formate produced during glycolysis via an enzyme complex called formate hydrogen lyase (FHL) [48]. Figure 5 depicts the role of the FHL enzyme complex in producing bioH_2 using formate as feedstock.

FHL enzyme complex consists of membrane-bound hydrogenase and formate dehydrogenase and many gram-negative bacteria like *E. coli*, *Salmonella* species, and *Klebsiella* that are known to exhibit the FHL activity. The fate of formate so produced is dependent upon the bacterial physiological environment and pH. Formate, which contains about one third of the carbon energy, is converted into molecular H_2 based on the following equation:

$$HCOO^- + H_2O \rightarrow HCO_3^- + H_2 \quad \Delta G^\circ = +1.3\ KJ/mol \tag{2}$$

E. coli has been found to utilize two H_2 metabolisms: the first one is the production of H_2 during mixed acid fermentation at slightly acidic pH, and the second metabolism is an uptake of H_2 along with quinone reduction [49]. *E. coli* utilizes four types of hydrogenase isoenzymes, viz. Hyd-1 and Hyd-2, which are involved in the uptake of H_2 in the periplasm and are encoded by *hya* and *hyb* operon, respectively, and Hyd-3 and Hyd-4, which are present at the cytoplasmic sites encoded by *hyc* and *hyf* operon, respectively [48]. Hyd-3 is bidirectional in nature and is involved in both H_2 uptake and its formation. It works in slightly acidic pH and initiates H_2 formation from formate via the FHL-1 enzyme complex. Hyd-3 further has one

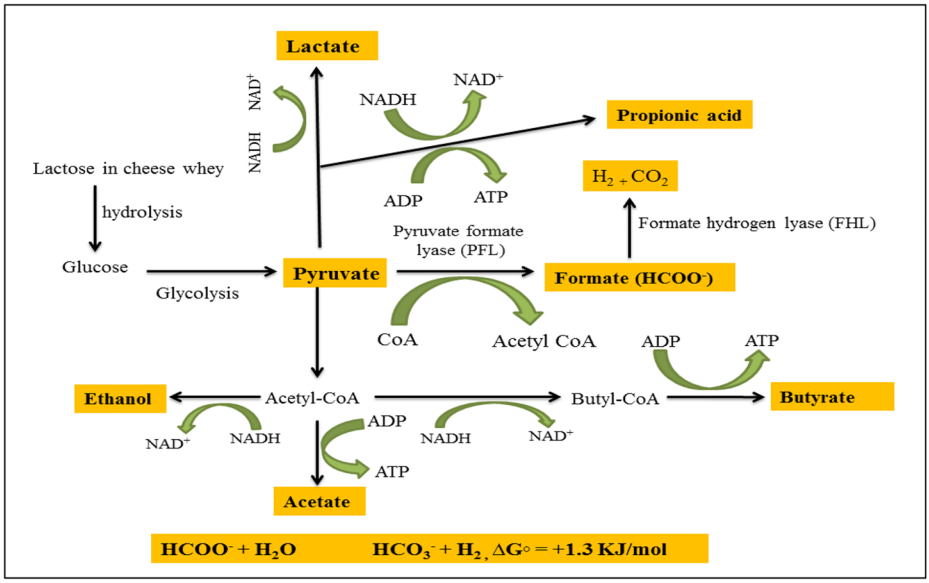

Fig. 5 Molecular bioH_2 production in facultative anaerobe

larger subunit and one smaller subunit encoded by *hycf* and *hycg*, respectively, which play a role during an integral transfer of electron. The expression of Hyd-4 is generally not significant, but it has also been known to produce H_2 in alkaline conditions as part of the FHL-2 enzyme complex [50].

BioH$_2$ production by DF of CW

H_2-producing microorganisms like facultative anaerobes (e.g., *Enterobacter* sp.) and obligate anaerobes (e.g., *Clostridium* sp.) carry out the process of DF. During DF, organic substrates, mainly carbohydrates, are oxidized by microbes to generate electrons that pass through a series of electrons carriers to H^+, which act as an electron acceptor and produce molecular H_2 to maintain electrical neutrality. Depending upon the mechanism used, further end products are soluble metabolites (acetic acid, butyric acid, lactic acid, and ethanol) [25]. It has been reported that only one third of the total energy stored in the organic biomass such as CW, food waste, and lignocellulosic feedstock is converted into bioH_2. The rest of the energy stored in the feedstock is converted into some useful metabolites in the form of fermentative liquid waste (FLW). During CW-based DF, pH and temperature are one of the critical parameters that should be maintained throughout the reaction as they affect the activity of hydrogenase enzyme, metabolic pathway, and production rate of H_2. The presence of lactic acid bacteria in the CW inhibits the production of bioH_2 during DF. Therefore, it is recommended to heat the CW sample at 85°C for around 30 min before autoclaving [41]. There are many studies that depict the batch fermentation of CW to produce bioH_2 by using various bacterial cells in suspension culture, as shown in Table 1.

Studies have been done to maximize bioH_2 production using different mixed microbial cultures and seed sludge from the upflow anaerobic sludge bioreactor (UASB) reactor mostly in mesophilic conditions (30–37°C) and within the pH range of 4–6 in different reactor configurations. Working with the CW, Neves et al. [51] produced bioH_2 in an anaerobic fluidized bed reactor (AFBR) having a working volume of 0.9 L. The fermentation was performed at three different organic load rates (OLRs) of 8.7 kg COD m^{-3} d^{-1}, 53.2 kg COD m^{-3} d^{-1}, and 101.7 kg COD m^{-3} d^{-1} corresponding to hydraulic retention time (HRT) of 8 h, 6 h, and 4 h, respectively. A decrease in H_2 yield was observed on increasing OLR with highest H_2 yield of 2.56 ± 0.62 mol mol^{-1} carbohydrate obtained at OLR of 53.25 kg COD m^{-3} d^{-1}. In another work, the authors used CW permeate for DFBP by using granular sludge as inoculum source. They obtained H_2 yield of 148 mmol H_2 L^{-1} day^{-1} with optimum nutrient concentration as follows: lactose from CW permeate: 20 g L^{-1}, ferrous sulfate: 0.6 g L^{-1}, ammonium sulfate: 1.5 g L^{-1}, and magnesium sulfate: 1.28 g L^{-1} [52]. Table 2 suggests detailed results so far on CW-based bioH_2 production system operated in continuous stirred-tank reactor (CSTR), UASB, and packed bed reactors along with their process parameters.

However, Lima D et al. [53] were able to produce more H_2 yield by using CW-based AnSBBR for bioH_2 generation as compared to conventional bioreactors such as CSTR and UASB. An anaerobic mixed culture containing mostly *Clostridium* sp. was immobilized on inert support matrix made up of polyethylene. Effect of feeding time, temperature, and influent concentration on bioH_2 production was analyzed, and they were able to get H_2 productivity and yield of 660 mL of H_2 L^{-1} d^{-1} and 0.80 mol of H_2 mol^{-1} lactose, respectively, at an influent concentration of 5.4 g COD L^{-1}. When CW fermentation is carried out in CSTR reactor having a working volume of 3.6 L at fixed HRT of 24 h and average OLR of 29 ± 4 g

Table 1 Studies on batch fermentation of CW for bioH_2 production

Inoculum	Working volume of bioreactor (L)	Process parameters		End products obtained	H_2 yield	Refs
		Temp (°C)	pH			
Anaerobic granular sludge	0.08	37	7.5	Acetic and butyric acid	3.6 mol H_2 mol^{-1} lactose	[86]
E. coli ΔhycA Δlacl	0.12	37	7.5	Acetic and butyric acid	2.74 mol mol^{-1} lactose	[87]
Anaerobic granular sludge	0.08	37	7.5	Butyric acid	1.8 mol mol^{-1}lactose	[88]
Anaerobic granular sludge	0.15	55	-	-	111 mL g^{-1} total sugar	[89]
Cow dung compost	0.8 and 1.8	39 ± 1	5.5–8.5	Lactic, formic, propionic, butyric, and succinic acid	171.3 NL kg^{-1} TOC	[90]
Anaerobic sludge	-	30	-	Acetic and butyric acid	15.33 mmol g−1 COD	[91]
Heat-treated anaerobic sludge	0.25	35 ± 1	5.0 ± 0.4	Acetic, lactic, propionic, and butyric acid	94.2 L kg^{-1} VS	[92]
Clostridium sp. IODB-O3	0.05	37	8.5	Lactic acid and butyric acid	6.35 ± 0.2 mol mol^{-1} lactose	[93]
Mixed microbial culture (*Clostridium* sp., *Lactobacillus* sp., and *Enterobacter* sp.)	0.7	30	7.0	Acetic and butyric acid	168.27 mmol L^{-1} d^{-1}	[94]
Bacterial consortia	0.7	30	7.0	Acetic, lactic, propionic, butyric acid, ethanol	3.9 mol mol^{-1} substrate	[52]
Anaerobic sludge	0.2	44.9	5.5–6.0	-	3.21 mol mol^{-1} glucose	[95]
Bacterial consortia	0.7	30	7.0	Acetic acid	3.21 mol mol^{-1} glucose	[52]
Lactobacillus acidophilus ATCC 4356	0.9	37	6.5	Propionic, acetic, butyric, pyruvic, formic, and lactic acid	1665 mL L^{-1}	[96]
Enterobacter asburiae	0.11	25.6	7.2	Ethanol, acetic, and formic acid	1.19 ± 0.01 mol mol^{-1} lactose	[97]

Table 2 Studies on fermentative bioH_2 production from CW using CSTR and UASB bioreactors

Inoculum	Process	Working volume of bioreactor (L)	Operational parameters			H_2 yield/HPR	Refs
			HRT (h)	pH	T (°C)		
Sludge from a confectionery factory (*Lactobacillus casei*, *Clostridium ramosum*)	UASB	1.3	24	5	30	0.38 L L^{-1} h^{-1}	[98]
RCW	PBR	2.5	24	>5	30	1.1 mol mol^{-1} lactose	[99]
Sludge from UASB reactor	AFBR	0.77	6	6	30 ± 1	1.27 mol mol^{-1} lactose in AFBR1 and 1.1 mol^{-1}mol lactose in AFBR2	[100]
Heat-treated sludge from poultry	AFBR	0.77	4	-	30	1.33 mol mol^{-1} lactose	[101]
Anaerobic sludge	CSTR	3	72	4.5–5.5	35	12 L kg^{-1} COD	[102]
Thermophilic anaerobic sludge	AFBR	1.98	4	4–4.5	55	H_2 yield: 3.67 ± 0.59 mol mol^{-1} lactose HPR: 4.1 ± 0.2 L h^{-1} L^{-1}	[103]
Sludge from digester	CSTR	1.5	12	8.3	55 ± 2	H_2 yield: 152.2 mL g^{-1} volatile solid HPR: 215.4 mL L^{-1} d^{-1}	[104]
Anaerobic sludge	CSTR	3	9	5.5 ± 0.1	36 ± 0.5	0.185 mol mol^{-1} lactose	[25]
Compost from kitchen waste	CSTR	3.6	24	5.5	30	H_2 yield: 0.9 mol mol^{-1} lactose HPR: 0.8 L L^{-1} d^{-1}	[54]
Anaerobic sludge	ASTBR	-	24	6.8 ± 0.1	25	H_2 yield: 1.4 ± 0.7 mol mol^{-1} lactose HPR: 1.6 ± 0.7 L H_2 L^{-1} d^{-1}	[55]
Biomass from fermentor	AFBR	0.9084	6	-	24–30	H_2 yield: 2.56 mol mol^{-1} carbohydrate HPR: 0.80 ± 0.21 L h^{-1} L^{-1}	[51]

ASBR anaerobic sequencing batch reactor, *UASB* upflow anaerobic sludge bioreactor, *KWC* kitchen waste compost, *RCW* raw cheese whey, *PBR* packed bed reactor, *AFBR* anaerobic fluidized bed reactor, *ASTBR* anaerobic structured-bed reactor

COD L^{-1} d^{-1}, lower but stable bioH_2 yield of 0.9 mol mol^{-1} lactose was achieved with the absence of any sort of operational problems such as bed clogging and methanogenesis [54]. Blanco et al. [55] obtained a high bioH_2 yield of 1.4 ± 0.7 mol mol^{-1} lactose in an acidogenic anaerobic structured-bed reactor (ASTBR) at OLR of 24 kg COD m^{-3} d^{-1}. They suggested that irrespective of the fermentation system used, bacterial culture has a threshold OLR value, which directs the metabolic pathway toward VFA production.

Possible use of FLW for the circular economy

Effluents of DF process contain acetic acid, butyric acid, ethanol, 1,3-propanediol, succinic acid, propionic acid, ethanol, and other metabolites depending upon the type of feedstock used and its concentrations [56] as shown in Fig. 6.

These metabolites have great industrial application and are worth to be recovered. The choice of bacterial culture and bioprocess mode also affects the composition of DF effluent [57]. These metabolites carry the vast potential to be used for producing a wide range of value-added products. The metabolites can be used as raw material for producing PHA (bioplastics), biobutanol, methane, phosphate-solubilizing biofertilizers (PSBs), and further bioH_2 in integrated fermentation. The production of different metabolites during H_2 production can be extended to the H_2 refinery approach as in addition to H_2; several other metabolites are also being produced simultaneously [58]. The purification of different metabolites to get them in pure form is a major bottleneck as the purification method is quite expensive. Therefore, a proper cost analysis strategy should be planned to achieve the desired bioH_2 refinery approach in which the FLW coming out from the first reaction could be utilized as a possible substrate for another fermentation. The prerequisite for the bioH_2 refinery is that the process must be developed in such a way that the production of different metabolites should not hamper the yield of H_2.

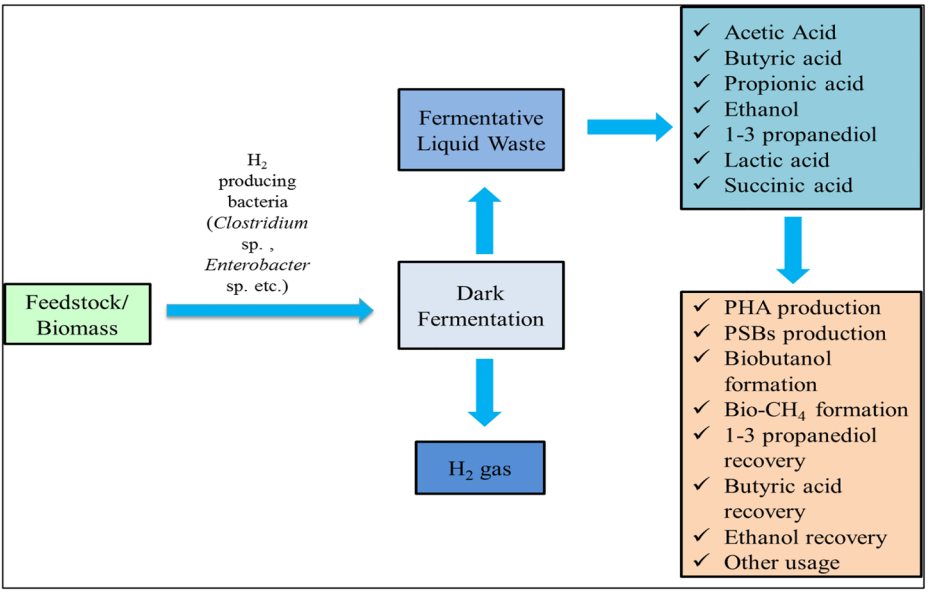

Fig. 6 Fermentative liquid waste and their promising applications

Sequential DF and PF strategy

The use of a hybrid fermentation system is another strategy to recover the maximum energy from carbon-rich CW. The yield of bioH_2 can be elevated by combining dark fermentative thermophilic reaction with PF by PNS bacteria. Sequential DF and PF is instead a holistic technique to supply the clean energy fuel by increasing the H_2 yield as compared to single-step dark and PF. Besides bioH_2 production, this augmented DF and PF provides a safe method for disposing of the CW within the environmental boundaries.

As mentioned earlier, during DF, a significant portion of the energy stored in CW in the form of lactose is being utilized in forming the DF effluents, which contain various VFAs along with bioH_2. These VFAs accumulate in the production medium, which inhibits bacterial growth, thereby decreasing the yield of bioH_2. So, electron-rich organic acids/alcohols present in the spent media of DF can be used again to produce further bioH_2 using PNS bacteria in PF (Fig. 7).

For effective production of bioH_2 by PF in sequential mode, there are some prerequisite conditions such as the concentration of NH_4^+ and VFA in DF effluent should be less than 40 mg L^{-1} and 2500 mg L^{-1}, respectively [59]. The concentration of NH_4^+ and VFA can be kept low by properly diluting spent media of DF, stripping of ammonia, and sterilizing and centrifuging DF effluent [60, 61].

Few studies have been published that involve the bioutilization of CW in two stages of DF and PF. In one of the studies done by Rai et al. [62], CW was utilized for producing bioH_2 in batch mode by using free and immobilized cells of *E. aerogenes* 2822 for DF and *Rhodopseudomonas* BHU 01 strain for the PF of the DF effluent containing dominantly acetic acid and butyric acid. H_2 yield and production rate by DF were increased from 2.04 mol mol^{-1} lactose (by free *E. aerogenes* cells) and 1.09 mmol L^{-1} h^{-1} to 3.50 mol mol^{-1} lactose and 1.91 mmol L^{-1} h^{-1} (by immobilized cells), respectively. During the PF, free *Rhodopseudomonas* BHU cells produced H_2 yield of 1.63 mol mol^{-1} acetic acid with a

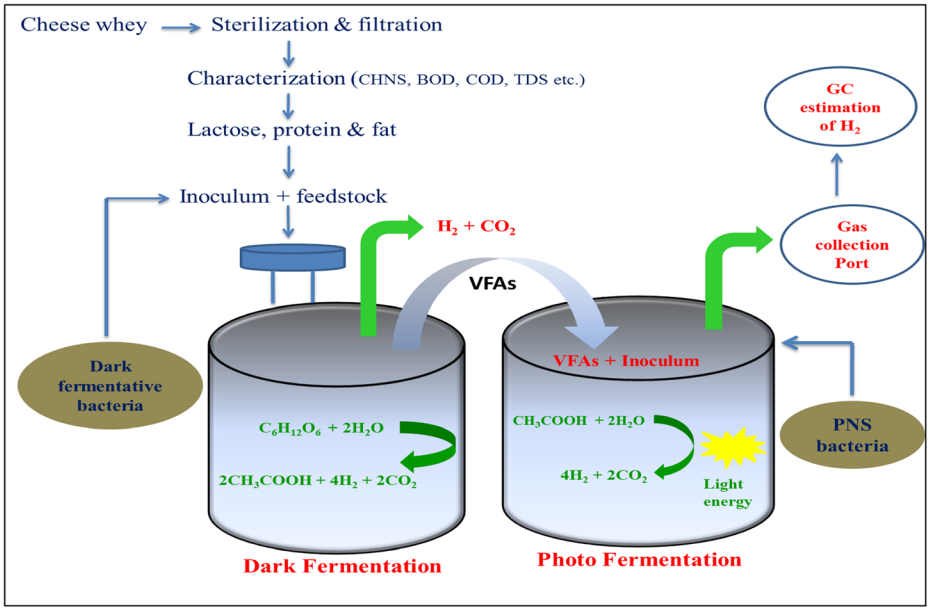

Fig. 7 Schematic diagram of proposed sequential dark-photo fermentation of CW

production rate of 0.49 mmol L^{-1} h^{-1} from DF effluent having 10 g L^{-1} of lactose, whereas immobilized cells of *Rhodopseudomonas* gave an improved yield of 2.69 mol mol^{-1} acetic acid. The overall H_2 yield by immobilized cells of both dark and PF was higher (5.88 mol mol^{-1} lactose) as compared to yield obtained by free cells (3.40 mol mol^{-1} lactose).

The effect of adding malic acid and dilution in CW effluent on bioH_2 production in two-stage anaerobic process has been studied, where the first stage comprises DF in thermophilic conditions by anaerobic microflora from a UASB reactor and second stage of PF by *R. palustris* DSM 127. This study summarizes that the presence of a higher amount of organic acids in fermentation broth did not favor the process. The addition of distilled water in the DF effluent helped the *R. palustris* cells to grow, by lowering the concentration of organic acids and nitrogen in fermentation effluent. However, the undiluted fermentation waste resulted in lower bioH_2 yield during PF. The overall bioH_2 yield was found to be between 2 and 10 mol mol^{-1} lactose [23]. Some of the recent studies involving sequential DF and PF for the production of bioH_2 have been outlined in Table 3.

The yield obtained by a sequential two-stage fermentation system is less than 50% of the total theoretical value, which may be because photofermentative PNS bacteria for the followed PF cannot accept acetic acid and butyric acid contained in the DF effluents as suitable feedstock for increased H_2 production. Therefore, another novel three-stage fermentative system has been developed for the production of H_2 and CH_4 with the main objective of higher yield of H_2. In this system, simple sugars present in the feedstock are first converted into a metabolic intermediate, mainly lactate, by using indigenous lactic acid bacteria without the production of H_2. During the second step, centrifuged supernatant of lactic acid effluents is used by photofermentative microorganisms for H_2 production followed by utilization of remaining effluents for CH_4 generation [63]. The different organic acids produced during DF are influenced by many factors such as pH, temperature, and nutritional requirements. Two-stage DF and PF has an advantage that the operational parameters can be optimized independently; therefore, optimization in the critical process parameters (viz. temperature, pH, inoculum age, the concentration of lactose in CW) using some statistical tools, viz. response surface methodology (RSM) and Gompertz equations, for each fermentation could positively enhance the total bioH_2 yield.

Statistical optimization of various physico-chemical parameters for high bioH_2 production rate

Significant work has been done in optimizing the important physico-chemical parameters of dark and PF by RSM to study the mutual interaction of different parameters and to establish the process parameters for fermentative bioH_2 production. RSM plays an essential role in scaling fermentative bioH_2 production from lab scale to pilot scale because it is an economically viable statistical method to select the bioprocess setpoint parameters (by screening technique of Plackett-Burman design) followed by the use of Box-Behnken design (BBD) or central composite design (CCD) to further investigate the effect of mutual interaction of fermentation parameters on response. Finally, an optimum response where the bioH_2 yield or production rate appears to be maximum is verified based on statistical experimental model building [64]. Further, based on the fermentation data achieved during RSM-based optimization studies at shake flask level, it becomes pivotal to conduct the large-scale bioH_2 production processes to know the actual variation from the optimum setpoint of bioprocess parameters.

Table 3 Studies on sequential DF and PF for efficient bioH_2 production

Substrate used	DFBI	PFBI	DF yield	PF yield	Overall productivity	Refs
Wheat powder solution	Anaerobic sludge	*Rhodobacter* sp. RV	1.87 mol mol^{-1} glucose	2.68 mol mol^{-1} glucose	4.55 mol mol^{-1} glucose	[105]
Sucrose	*C. butyricum* CGS5	*R. palustris* WP3-5	6.56 mol mol^{-1} sucrose	5.06 mol mol^{-1} sucrose	11.61 mol mol^{-1} sucrose	[106]
Cassava starch	Anaerobic mixed bacteria (mainly *Clostridium* species)	Immobilized mixed photosynthetic bacteria (mainly *R. palustris* species)	2.53 mol mol^{-1} hexose	3.54 mol mol^{-1} hexose	6.07 mol mol^{-1} hexose	[107]
Starch	Microbial consortium	*R. capsulatus* B10 and *R. sphaeroides* N7	1.4 mole mol^{-1} hexose	3.9 mole mol^{-1} hexose	5.3 mole mol^{-1} hexose	[108]
Wet biomass of *Arthrospira platensis*	*C. butyricum*	*R. palustris*	96.6 mL g^{-1} dry weight	243.4 mL g^{-1} dry weight	337.0 mL g^{-1} dry weight	[109]
Crude glycerol	*Klebsiella* sp. TR17	*R. palustris* TN1	5.74 mmol g^{-1} COD	0.68 mmol g^{-1} COD	6.42 mmol g^{-1} COD	[110]
Starch wastewater	Sludge immobilized on maghemite nanoparticles	*R. palustris*	104.75 ± 12.39 mL g^{-1} COD	-	166.83 ± 27.79 mL g^{-1} COD	[111]
Cassava ethanol wastewater	*C. butyricum*	*R. palustris*	23.6 mL g^{-1} COD	369.7 mL g^{-1} COD	386.6 mL g^{-1} COD	[112]
POME	*C. butyricum* LS2	*R. palustris*	0.784 mL mL^{-1} POME	2.86 mL mL^{-1} POME	3.064 mL mL^{-1} POME	[113]
Starch and glucose	*C. butyricum* NRRL-B-1024 and *E. aerogenes* NRRL-B-115	*R. palustris GCA009*	-	7.21 mmol H_2 g^{-1} COD	8.3 mmol g^{-1} COD	[114]
Corn stover	Sewage sludge	Mixed culture HAU-M1	22.4 m^3 d^{-1}	37.3 m^3 d^{-1}	59.7 m^3 d^{-1}	[6]
Glucose	Salt-tolerant consortia (mainly *Clostridium* spp.)	Consortia (includes *R. sphaeroides*, *R. palustris*, *Rhodovulum sulfidophilum*)	2.67 mol mol^{-1} glucose	3.11 mol mol^{-1} glucose	5. 78 mol mol^{-1} glucose	[115]
Chlorella sp. biomass	Anaerobic sludge	*R. sphaeroides* TISTR 1952	47.2 mL g^{-1} VS	125 mL g^{-1} VS	172.2 mL g^{-1} VS	[4]
Rice straw hydrolysate	*Bacillus cereus*	*Rhodopseudomonas rutila*	1.53 ± 0.04 mol mol^{-1} glucose	0.25 ± 0.04 mol mol^{-1} glucose	1.82 mol mol^{-1} glucose	[116]

POME palm oil mill effluent

Based on the literature survey, it has been suggested that full factorial design (FFD) and fractional factorial approach are necessary to study the all-possible combinations by changing certain variables together in a controlled way to study their effect on the output of a process, as compared to one factor at a time. Further, exploring second-order quadratic models such as BBD, CCD, and Taguchi methods for robust parameters and Doehlert design is preferably used to investigate the interactive effects of specific parameters, leading to maximum production of bioH_2, due to less number of experiments required to get the optimum response as compared to 3^Ndesign.

First-order polynomial design (Plackett-Burman design, 2^K factorial design, and simplex design) is obtained by Eq. 3:

$$y = a_\circ + \sum_{i\approx 1}^{k} a_i x_i + \varepsilon \tag{3}$$

Second-order interaction models (CCD, BBD, and 3^k factorial) are preferably used in optimization study by fitting the second-order polynomial model as compared to first-order models as it suffers from the lack of fit, resulting from the interaction between independent factors and surface curvature. Second-order polynomial design (also known as response surface model) should contain the level of variables and quadratic terms based on the following equation:

$$y = a_\circ + \sum_{i\approx 1}^{k} a_i x_i + \sum_{i\approx 1}^{k}\sum_{j\approx 1}^{k} a_{ij} x_i x_j + \sum_{i\approx 1}^{k} a_{ii} x_i^2 \tag{4}$$

where a_0 is the tuning parameter and x_i and x_j are the model variables.

The BBD design requires at least three levels for each factor, which are rotatable in nature. CCD contains a 2k factorial design (complete or fraction) having coded levels as +1 and −1, n_o center points, and augmented axial points or star points, which are at a distance of $+\alpha$ and $-\alpha$ on each axis. The choice between BBD and CCD models in case of optimizing operational parameters for optimum bioH_2 production depends on the experimental region; i.e., if extreme points (star points and corner points) are to be avoided, then BBD should be preferred as it excludes the extreme combination of independent variables, which seem to be not suitable for the growth of dark fermentative bacteria and PNS bacteria. Otherwise, both models work well.

Basak N et al. [16] have used FFD for optimizing the photofermentative bioH_2 production parameters to study the mutual effects of DL malic acid concentration, L glutamic acid concentration, and temperature on average H_2 production rate. In this particular work, authors used only FFD for optimizing bioH_2 production; hence, we used the FFD data of this study to further perform the statistical optimization of medium composition by BBD and CCD under RSM. Table 4 shows the experimental variables and their assigned levels for three optimization models.

A comparison between the FFD matrix, BBD, and CCD models in terms of the level of variables and experimental design in uncoded units has been shown in Table 5.

As evident from Table 5, the last three combinations for BBD are the center points, and other points include one of the factors for the BBD model as 0 along with + or – combination for the rest of the two factors.

By using software Minitab 16.0, quadratic regression equation in coded form and uncoded form was developed based on independent variables for FFD model, BBD, and CCD as shown below.

Table 4 Experimental variables and their level assigned for optimizing bioH_2 production

Model	FFD			BBD			CCD				
Independent variables	Parameter values			Parameter values			Axial point	Parameter values			Axial point
	−1	0	+1	−1	0	+1	−1.68	−1	0	+1	+1.68
DL-malic acid concentration (g L^{-1}, x_1)	1.34	2.01	2.68	1.34	2.01	2.68	0.88	1.34	2.01	2.68	3.14
L glutamic acid (g L^{-1}, x_2)	0.15	0.3	0.45	0.15	0.3	0.45	0.05	0.15	0.3	0.45	0.55
Temperature (°C, x_3)	27	32	37	27	32	37	23.6	27	32	37	40.41

Table 5 Experimental design points for FFD, BBD, and CCD in coded form, observed, and predicted values for H_2 production rate

FFD						BBD					CCD				
Run	Coded value			AHPR	[a]AHPR	Coded value			[a]AHPR	AHPR	Coded values			[a]AHPR	[a]AHPR
	x1	x2	x3	Actual values	Predicted value	x1	x2	x3	Actual values	Predicted value	x1	x2	x3	Actual values	Predicted value
1	−1	−1	−1	4.89	4.85	−1	−1	0	5.05	5.08	−1	−1	−1	4.89	4.94
2	−1	−1	0	5.05	5.11	+1	−1	0	6.46	6.54	+1	−1	−1	6.3	6.12
3	−1	−1	+1	4.79	4.74	−1	+1	0	5.10	5.04	−1	+1	−1	4.84	5.26
4	−1	0	−1	5.16	5.19	+1	+1	0	6.67	6.66	+1	+1	−1	6.25	6.44
5	−1	0	0	5.42	5.44	−1	0	−1	5.16	5.17	−1	−1	+1	4.79	4.46
6	−1	0	+1	5.00	5.06	+1	0	−1	6.77	6.74	+1	−1	+1	6.15	5.59
7	−1	+1	−1	4.84	4.82	−1	0	+1	5.00	5.05	−1	+1	+1	4.69	4.73
8	−1	+1	0	5.10	5.07	+1	0	+1	6.56	6.57	+1	+1	+1	6.04	5.85
9	−1	+1	+1	4.69	4.68	0	−1	−1	7.45	7.43	+1.68	0	0	6.23	6.56
10	0	−1	−1	7.45	7.39	0	+1	−1	7.40	7.47	−1.68	0	0	4.83	4.63
11	0	−1	0	7.60	7.63	0	−1	+1	7.34	7.29	0	+1.68	0	6.21	5.84
12	0	−1	+1	7.34	7.25	0	+1	+1	7.29	7.33	0	−1.68	0	4.85	5.35
13	0	0	−1	7.71	7.74	0	0	0	7.88	7.93	0	0	+1.68	4.55	5.06
14	0	0	0	7.92	7.97	0	0	0	7.92	7.93	0	0	−1.68	6.33	5.95
15	0	0	+1	7.50	7.59	0	0	0	7.97	7.93	0	0	0	7.81	7.86
16	0	+1	−1	7.40	7.38	[a]AHPR - average H_2 production rate expressed in mL L^{-1} h^{-1}					0	0	0	7.84	7.86
17	0	+1	0	7.55	7.6						0	0	0	7.92	7.86
18	0	+1	+1	7.29	7.21						0	0	0	7.88	7.86
19	+1	−1	−1	6.30	6.34						0	0	0	7.85	7.86
20	+1	−1	0	6.46	6.56						0	0	0	7.97	7.86
21	+1	−1	+1	6.15	6.17										
22	+1	0	−1	6.77	6.7										
23	+1	0	0	7.08	6.92										
24	+1	0	+1	6.56	6.52										
25	+1	+1	−1	6.25	6.36										
26	+1	+1	0	6.67	6.57										
27	+1	+1	+1	6.04	6.16										

In coded form,
For FFD,

$$Y_{HPR} = 7.97148 + 0.74111x_1 - 0.01111x_2 - 0.07833x_3 + 0.0125x_1x_2 - 0.01333x_1x_3 - 0.00917x_2x_3 - 1.79444{x_1}^2 - 0.35444{x_2}^2 - 0.30944{x_3}^2 \quad (5)$$

For BBD,

$$Y_{HPR} = 7.9233 + 0.7687x_1 + 0.0200x_2 - 0.0738x_3 + 0.0400x_1x_2 - 0.0125x_1x_3 - 0.0000x_2x_3 - 1.8004{x_1}^2 - 0.3029{x_2}^2 - 0.2504{x_3}^2 \quad (6)$$

For CCD,

$$Y_{HPR} = 7.874 + 0.577x_1 + 0.145x_2 - 0.264x_3 - 0.001x_1x_2 - 0.014x_1x_3 - 0.014x_2x_3 - 0.801{x_1}^2 - 0.801{x_2}^2 - 0.833{x_3}^2 \quad (7)$$

In uncoded form,
For FFD,

$$Y_{HPR} = -24.2693 + 17.265x_1 + 9.51889x_2 + 0.788178x_3 + 0.124378x_1x_2 - 0.00398x_1x_3 - 0.01222x_2x_3 - 3.9974{x_1}^2 - 15.7531{x_2}^2 - 0.0123778{x_3}^2 \quad (8)$$

For BBD,

$$Y_{HPR} = -21.62 + 17.271x_1 + 7.41x_2 + 0.634x_3 + 0.398x_1x_2 - 0.0037x_1x_3 - 0.0000x_2x_3 - 4.0107{x_1}^2 - 13.46{x_2}^2 - 0.01002{x_3}^2 \quad (9)$$

For CCD,

$$Y_{HPR} = -37.44 + 8.71x_1 + 22.94x_2 + 2.093x_3 - 0.01x_1x_2 - 0.0041x_1x_3 - 0.018x_2x_3 - 1.785{x_1}^2 - 35.61{x_2}^2 - 0.03332{x_3}^2 \quad (10)$$

The goodness-of-fit statistic between predicted and experimental average H_2 production rate (mL L^{-1} h^{-1}) of three different models, viz. FFD, BBD and CCD, was compared based on "predicted squared regression statistic (R^2)" value and "adjusted R-squared" value and regression equation pattern.

Further, comparative analysis of variance (ANOVA) shows the significance of all the three quadratic models in terms of linear, quadratic, and two-level interactions (Table 6).

The *F*-values for FFD, BBD, and CCD are 451.27, 340.04, and 19.81, respectively, which imply that FFD and BBD models are significant and CCD was considered to be insignificant, and there are 0%, 0.05%, and 0.0% chances for FFD, BBD, and CCD, respectively, that "model *F*-value" for these three models occurs due to the noise. The insignificant nature of CCD model was due to the presence of axial points ($+\alpha$ and $-\alpha$ having values of +1.68 and −1.68, respectively; see Table 4) on each axis, which were extreme condition for the growth of bacteria and for bioH_2 production using *R. sphaeroides* O.U.001 cells (for, e.g., x_3, temperature of 40.41°C, see Table 5). Therefore, some authors have excluded the experiments with axial points during optimization of bioH_2-producing parameters [65].

Lack-of-fit *F*-value compares the lack of fit variance with that of pure error variance. "Lack-of-fit *F*-values" for FFD and BBD were 59.66 and 96.11, respectively, which imply that it is insignificant and model fits the data well, proven by the *P*-values of 0.0167 and 0.0 for FFD and CCD, which tells that there are 1.67% and 0% chances that "model *F*-value" occurred due to noise. For CCD, the "lack of fit" was significant ($P > 0.05$). From Table 6,

Table 6 ANOVA results for quadratic response models of H_2 production rate for three optimization models

Model term	df[1]			Adj SS[2]			Adj MS[3]			*F*-value[4]			*P*-value[5]		
	FFD	BBD	CCD	FF	BBD	CCD	FFD	BBD	CCD	FFD	BBD	CCD	FFD	BBD	CCD
Model	9	9	9	30.6526	16.8880	29.5708	3.4058	1.8764	3.28564	451.27	340.04	19.81	0.0	0.0005	0.000
x_1 (malic acid)	1	1	1	9.8864	4.7278	4.5520	9.8864	4.7278	4.55196	1309.95	856.75	27.44	0.0	0.000	0.000
x_2 (glutamic acid)	1	1	1	0.0022	0.0032	0.2863	0.0022	0.0032	0.28626	0.29	0.58	1.73	0.594	0.481	0.218
x_3 (temperature)	1	1	1	0.1104	0.0435	0.9509	0.1104	0.0435	0.95087	14.63	7.89	5.73	0.001	0.038	0.038
x_1x_2	1	1	1	0.0019	0.0064	0.0000	0.0019	0.0064	0.00001	0.22/	1.16	0.00	0.625	0.331	0.993
x_1x_3	1	1	1	0.0021	0.0006	0.0015	0.0021	0.0006	0.00151	0.28	0.11	0.01	0.602	0.750	0.926
x_2x_3	1	1	1	0.0010	0.0000	0.0015	0.0010	0.0000	0.00151	0.13	0.00	0.01	0.719	1.000	0.926
x_1^2	[a]1	1	1	19.9202	11.9686	9.2494	19.9202	11.9686	9.24943	2559.93	2168.88	55.75	0.0	0.000	0.000
x_2^2	[a]1	1	1	0.7538	0.3388	9.2494	0.7538	0.3388	9.24943	99.88	61.40	55.75	0.0	0.001	0.000
x_32	[a]1	1	1	0.5745	0.2315	9.9988	0.5745	0.2315	9.99877	76.13	41.96	60.27	0.0	[b]0.001	[c]0.000
R squared	-			-			0.9958	0.9984	0.9469	-			-		
Adj R squared	-			-			0.9936	0.9954	0.8991	-			-		
Pred R-squared	-			-			0.9892	0.9872	59.99	-			-		
Lack of fit	7	3	5	0.1253	0.0235	1.6419	[a]0.0179/[b]0.0078/[c]0.32838			59.66	96.11	3.86	0.0167	0.000	0.213
Pure error	10	2	5	0.0030	0.0041	0.0171	[a]0.0003/[b]0.0020/[c]0.00342			-			-		
Correlation total	26	14	19	30.7809	16.9156	31.2298	-			-			-		

1 df degrees of freedom, *2 Adj SS* sum of square, *3 Adj MS* mean square, *4 F-value* Fisher-Snedecor distribution value, *5 P-value* Prob>F

R^2 values for FFD, BBD, and CCD were calculated to be 99.58%, 99.84%, and 94.69%, respectively, which prove that the mathematical models chosen demonstrate a good correlation between the predicted and observed values for H_2 production rate. For the model terms to be significant, *P*-values should be less than 0.0500 [66]. Based on the *P*-values from Table 6 obtained for three models, x_1 (DL malic acid) and x_3 (temperature) were significant ($P < 0.05$); x_2 (L glutamic acid) was not significant ($P > 0.05$); and x_1^2, x_2^2, and x_3^2 were significant ($P < 0.05$), while the interactions between x_1 (DL malic acid) and x_2 (L glutamic acid), x_1 (DL malic acid) and x_3 (temperature), and x_2 (L glutamic acid) and x_3 (temperature) were not significant ($P > 0.05$).

Rao et al. [67] optimized the concentration of total carbohydrate present in CW along with temperature and pH for improved bioH_2 production by *E. aerogenes* cells in a double-walled cylindrical bioreactor. BBD matrix of RSM gave maximum hydrogen production rate of 24.7 mL L^{-1} h^{-1} at optimum values of CW 32.5 g L^{-1}, temperature of 31°C, and pH of 6.5. In a recent study, Zainal BS et al. [68] studied the bioH_2 production from palm oil mill effluent (POME) using anaerobic sludge from a pond as inoculum. They used the CCD matrix to investigate the effect of three independent variables, viz. inoculum to substrate ratio, reaction temperature, and reaction time, on molar bioH_2 yield. Optimum H_2 yield of 28.47 mL g^{-1} COD was obtained with an inoculum-to-substrate ratio of 40:60, reaction temperature of 50°C, and reaction time of 8 h. Sagir E et al. [69] obtained maximum bioH_2 yield of 7.8 ± 0.1 mol mol^{-1} glucose and production rate of 21 ± 0.25 mmol L^{-1} from immobilized cells of *R. capsulatus* JP91 in sequential DF and PF by utilizing BBD to optimize three important key process variables (O_2 concentration, inoculum concentration, and glucose) at optimum concentrations of 4.5%, 62.5% v/v, and 6 mM, respectively. This study claimed to produce maximum H_2 yield until now using an immobilized cell system. Hidalgo et al. [65] demonstrated the possible use of CW and wheat straw hydrolysates (WSHs) individually and in codigestion approach for optimizing the DFBP by using CCD matrix. Maximum bioH_2 yield of 5724.5 mL L^{-1} was obtained at an optimum substrate concentration of 30 g L^{-1} (5 g L^{-1} WSH and 25 g L^{-1} CW), pH of 7.25, and temperature of 26.6°C. Mahata C et al. [70] optimized dark fermentative bioH_2 yield by utilizing starchy wastewater along with groundnut deoiled cake with the help of pretreated acidogenic bacterial consortia. Optimization in pH value, groundnut deoiled cake concentration, and temperature was done by performing CCD design of RSM along with artificial intelligence such as artificial neural network and support vector machine. At optimum operating pH of 6.75, groundnut deoiled cake concentration of 16.16 g L^{-1}, and temperature of 37.55°C, they observed 2.1-fold increase in bioH_2 yield by using support vector machine–based optimization model as compared to unoptimized conditions. Many authors have tried to optimize the operational parameters responsible for higher fermentative bioH_2 yield using different RSM models, and some of the recent developments have been mentioned in Table 7.

The studies in Table 7 highlight the pivotal role of RSM in optimizing fermentative H_2 production processes at shake flask level by using simple sugars and organic waste materials. In a recent study by Hassan et al. [71], optimization in pH, carbon-to-nitrogen ratio, and light intensity during PF has been done successfully with the help of RSM and three-factor three-level BBD matrix. They reported a maximum bioH_2 production rate of 41.74 mL L^{-1} h^{-1} from DL malic acid by a mesophilic fermentative process in the presence of *R. sphaeroides* 158 DSM under the optimum factors determined by JMP statistical discovery™ software (13.1.0).

Table 7 Summary of optimization studies for fermentative bioH_2 production system in different modes

Bacterial strain	Feedstock and operation mode	Working volume of reactor (L)	Operational parameters studied with its optimum value	Model evaluated	H_2 yield/HPR	Refs
Rhodobacter sphaeroides O.U.001	DL malic acid, batch (PF)	1	DL malic acid concentration (2.012 g L^{-1}), L glutamic acid concentration (0.297 g L^{-1}), temperature 32°C	CCD	HPR: 7.97 mL L^{-1} h^{-1}	[16]
Anaerobic seed sludge	Dairy wastewater, batch (DF)	-	Ultrasonic density (0.08 W mL−1) Ultrasonic time (9 min)	CCD	H_2 yield: 15.33 mmol g^{-1} COD SHPR: 31.38 mmol g^{-1} VSS d^{-1}	[91]
R. sphaeroides NMBL-02 and *E. coli* NMBL-04	Malate, batch (PF)	0.12	Malate concentration (3.948 g L^{-1}), pH (5.603), iron concentration (0.312 g L^{-1})	BBD	HPR: 2046 mL L^{-1}	[117]
Seed sludge	SCB, batch (DF)	0.1	Substrate concentration (22.77 g total sugar L^{-1}), inoculum:substrate ratio (0:31), substrate:buffer ratio (4:31)	CCD	HPR: 6980 mL L^{-1}	[118]
Anaerobic sludge	Glycerin, batch (DF)	0.1	Glycerin concentration (0.5 g L^{-1}), pH (5.5), VSS (8.7 g L^{-1})	CCD	H_2 yield: 2.44 mol mol^{-1}glycerin	[119]
Anaerobic sludge	CW, batch (DF)	0.5	Inoculum-substrate ratio (1.44 g VS g^{-1} TOC) pH (5.5)	Spearman's analysis	H_2 yield: 371 L kg^{-1} TOC	[120]
Enterobacter aerogenes PTCC 1221	Rice straw, batch (DF)	0.02	Temperature (180°C), residence time (30 min), ethanol conc. (45%, v/v)	CCD	H_2 yield: 19.73 mL g^{-1} straw	[121]
Anaerobic digested seed	Molasses, batch (DF)	0.08 and 0.8	For $BBD_{0.08}$: inoculum size (34.84%), HRT (41.84 h), molasses concentration (100 g L^{-1}) For $BBD_{0.8}$: inoculum size (32.71%), HRT (38.44 h), molasses concentration (100 g L^{-1})	BBD	H_2 yield: 0.99 mol mol^{-1} sucrose for $BBD_{0.08}$ and 0.70 mol mol^{-1} sucrose for $BBD_{0.8}$	[122]
Rhodobacter sphaeroides 158 DSM	DL malic acid, batch (PF)	0.12	C/N ratio (27.5), pH (7.4), light intensity (126 W m^{-2})	BBD	HPR: 41.74 mL L^{-1} h^{-1}	[71]
R. sphaeroides JP91	Glucose, batch (PF)	0.04	Glucose conc. (1.08 g L^{-1})	BBD	H_2 yield:	[69]

Table 7 (continued)

Bacterial strain	Feedstock and operation mode	Working volume of reactor (L)	Operational parameters studied with its optimum value	Model evaluated	H_2 yield/HPR	Refs
			Oxygen conc. (4.5%) Inoculum conc. (62.5%,v/v)		7.8 ± 0.1 mol mol^{-1} glucose HPR: 21 ± 0.25 mmol L^{-1}	
Rhodopseudomonas palustris	DPOME, batch (PF)	1	Light intensity (250 W m^{-2}), agitation rate (200 rpm), dilution of DPOME (30%)	3^k BBD	H_2 yield: 3.07 ± 0.66 mol mol^{-1} acetate	[66]
Anaerobic sludge	CW and WSH, batch (DF)	0.11	Temperature (26.6°C), pH (7.25), CW: 25 g L^{-1},WSH: 5 g L^{-1}	CCD	HPR: 5724.5 mL L^{-1}	[123]
E. aerogenes	Sago wastewater, batch (DF)	1	Yeast extract conc. (4.8 g L^{-1}) temperature (31°C) inoculum conc. (5%,v/v)	CCD	H_2 yield: 7.42 mmol mol^{-1} glucose	[124]
Pseudorhodobacter sp. (KT163920)	Glucose, batch (DF)	0.12	Temperature (29°C), initial pH (6.86), glucose concentration (28.4 g/$dm^{3)}$	CCD	H_2 yield: 1.7 mol mol^{-1} glucose	[125]
Anaerobic sludge	Wheat powder, immobilized batch reactor (DF)	0.2	Temperature (44.9°C), sugar concentration (10 g L^{-1}), particle number (240)	BWD	H_2 yield: 3.21 mol H_2 mol^{-1} glucose, HPR: 73.3 mL h^{-1}	[95]
E. aerogenes 2822	CW, batch (DF)	1.5	CW conc. (32.5 g L^{-1}), temperature (31 °C), pH (6.5)	BBD	HPR: 24.7 mL L^{-1} h^{-1}	[67]
Enterobacter asburiae	CWP, batch (DF)	0.11	Temperature (25.6°C), pH (7.2), CWP (23 g L^{-1})	CCD	H_2 yield: 1.19 ± 0.01 mol mol^{-1} lactose HPR: 9.34 ± 0.22 mL L^{-1} h^{-1}	[97]

DF dark fermentation, *BBD* Box-Behnken design, *PF* photo fermentation, *PBD* Plackett-Burman design, *CCD* central composite design, *SCB* sugarcane bagasse, *VSS* volatile suspended solid, *DPOME* dark fermented palm oil effluent, *CW* cheese whey, *WSH* wheat straw hydrolysate, *BWD* Box-Wilson design, *CWP* cheese whey powder

Application of computational fluid dynamics simulation on bioH_2-producing bioreactors for higher substrate conversion efficiency

The computational fluid dynamics (CFD) simulation to the H_2-producing bioreactor at the lab scale for hydrodynamics study can help in scaling up the process more efficiently by removing the necessity of field test. CFD has been used in anaerobic fermentation to produce bioH_2 as the data produced based on process simulation about the turbulence, heat and mass transfer, and temperature gradient inside the bioreactor is vital with respect to microbial behavior of H_2-producing bacteria. Many studies have focused on producing bioH_2 in CSTR, granular sludge bed bioreactor, and sequencing batch reactor, but limited efforts have been done to study the flow pattern of fermentation broth and fraction of multiphase (gas-liquid-solid) inside the bioreactor.

The overall efficiency of PBR can be analyzed by modern CFD, which is based on a suitable mathematical model and is used to study the hydrodynamics behavior (velocity distribution, shear strain rate, temperature distribution of media) and heat and mass transfer inside the PBR [72]. In addition to the PBR, CFD technology has proven to be an efficient tool in optimizing and designing a suitable bioreactor for producing bioH_2 in continuous mode by examining the microorganism growth and pattern of fluid flow of almost every region inside the reactor including the region covered by baffles and impeller [73].

Strategy for CFD numeric simulation

A typical CFD simulation study using ANSYS-Fluent model comprises the following steps:

(i) Pre-processing step, which involves the creation of a specific geometry by applying symmetrical boundary conditions and generation of mesh. The boundary conditions (tank surface, impeller size, draft) should be defined first before meshing in ANSYS-Fluent. The mesh is generally created in the form of high-quality grids, which are useful for steady-state approximation. Studies confirm that the PBRs containing radial or axial flow impellers have used moving reference frame (MRF) for creating the mesh. MRF technology divides the reactor geometry into two domains, static reference frame (SRF) domain and inner rotatory reference domain [74].

(ii) After the creation of mesh geometry, they are exported to the ANSYS-Fluent to solve the differential equations governing the flow of fermentation media inside the PBR. The mass, momentum, and energy balance are calculated based on inter-phase momentum equations. However, the equation accountable for energy conservation can be ignored if the temperature inside the PBR is constant.

(iii) Post-processing of simulation results for further data analysis. Fluid flow in PBR is visualized using some methods like vector plots and contour plots for heat transfer pattern and pathlines. Some important software used for post-processing are ANSYS CFD-Post, Field View, and ParaView.

Brindhadevi et al. [75] explored the critical role of HRT and OLR in optimized bioH_2 production by applying 2-D CFD simulation of gas-liquid-solid phase in bioH_2 producing CSTR system at different values of HRT/OLR. The flow behavior of each phase was analyzed using the Eulerian fluid approach. Distribution of velocity and movement of the sludge particle inside the reactor were found to be affected by the nature of the gas bubble formed in the reactor. The optimum fluid flow behavior leading to better microbial growth and good substrate conversion efficiency was obtained at HRT of greater than 2 h.

In recent years, CFD-based simulation strategy has emerged as an important analytical framework for the researchers throughout the globe to study the heat/mass transfer dynamics, fluid flow dynamics of fermentation liquid, and other biochemical processes of large-scale $bioH_2$ bioreactors. The successful scaling up of any fermentation process largely depends on the fluid flow, dissolved oxygen concentration, distribution of temperature inside the bioreactor, feedstock concentration, and pH. The most challenging tasks during a large-scale operation of $bioH_2$ fermenters are non-uniform fluid flow of fermentation media and inadequate supply of dissolved oxygen to the cells inside the bioreactor [74]. To carefully study the abovementioned parameters, CFD simulation tools have been applied to scale up the bioprocess by numeric modeling in different configurations of bioreactors such as anaerobic biofilm bioreactor, plug flow digester, photobioreactor, and CSTR, thereby solving many scale-up and complex geometry issues before performing the experiments at large scale. The significance of CFD tools in moving from hit-and-trial procedures to scale up of $bioH_2$ bioreactors has been specifically discussed together with the requirement of a multiphase flow model [76]. In view of the above, Wang Xu et al. [77] compared laboratory-scale fermenter (17 L) and an industrial-scale CSTR (140,000 L) in terms of shear strain and fluid velocity of fermentation liquid and tried to scale up industrial-CSTR using CFD-based model. The outcomes in terms of hydrodynamics assessment highlighted the importance of the stagnation zone and velocity field as the crucial parameters for optimizing industrial CSTR. The shear strain rate of laboratory-scale CSTR above the impeller was found to be more as compared to industrial CSTR.

As a matter of fact, the CFD-based simulation model has been applied to predict the flow patterns of reaction liquid in CSTR for $bioH_2$ generation. Recently, CFD, ANSYS Fluent 14.5, was used by Navarro et al. [78] to investigate the flow pattern generated by using two different geometries of fermenter's impeller, viz. pitched blade PB4 and Rushton impeller. Pitched blade PB4 impeller was found to be most suitable for the maximum consumption of feedstock, thereby giving maximum $bioH_2$ productivity of 440 mL L^{-1} h^{-1}.

Effect of baffle angles (30°, 35°, 40°, 45°, 50°, and 55°) on the separation efficiency of the three-phase separator in an expanded granular sludge bed reactors (EGSBs) was studied by Pan et al. [79] using three-dimensional CFD simulation. It was observed that at baffle angle of 40°, loss of sludge from the reactor was smallest. Also, the fraction of gas volume was found to be increasing or decreasing the baffle angle. In another study done by PC et al. [80], the Euler-Euler model with multiple reference frames was investigated to find out the flow behavior of gas, liquid, and solid phase inside the horizontal CSTR system leading to higher production of $bioH_2$. Post-processing of CFD-simulated data validates the strong relation between agitation speed and optimum $bioH_2$ yield. The agitation speed was calculated based on the analysis of shear strain rate, velocity gradient, and volume fraction of biogas inside the bioreactor. The agitation speed of 50 was observed as the optimum value for getting maximum $bioH_2$ yield of 62 L D^{-1} along with the separation of three phases in a bioreactor.

In case of PF, the distribution of light inside the bioreactor plays an important role, which is also related to heat transfer. Effect of varying inlet fluid velocities on heat transfer and temperature distribution profile in a upflow baffle photo bioreactor (UBPB) has been studied by Zhang et al. [81] by using CFD-based simulation model. Most uniform temperature distribution throughout the length of PBR was found at a fluid velocity of 0.0036 m s^{-1}. The same group of authors were able to get satisfactory $bioH_2$ yield by performing CFD simulation of tubular PBR [82]. They studied the heat transfer and temperature distribution profile inside the PBR and highlighted light radiation as one of the important parameters

affecting temperature gradient distribution. Some of the recent studies involving the application of CFD-based simulation model for enhancing $bioH_2$ production on the basis of flow pattern analysis inside the bioreactor has been outlined in (Table 8).

Summary for possible future improvement

Despite tremendous R&D until now in this field, the significant obstacles such as incomplete utilization of available sugar present in CW, lower production rate of $bioH_2$, and lack of efficient bioreactors for producing $bioH_2$ remain to be overcome for developing a large-scale $bioH_2$ production system at economically lower cost. Carbohydrate-rich CW has proven to be an attractive substrate for fermentative $bioH_2$ production as it helps in the production of bioenergy along with effective removal of pollutant, but a clear understanding of suitable bioreactor design is necessary to optimize the critical operational parameters and scale up the $bioH_2$ production from lab scale to pilot scale.

Use of microbial consortium to degrade the complex biomass might improve the $bioH_2$ yield as compared to pure H_2-producing microbes. Also, in recent years, scientists have acquired decent progress in understanding the mechanism of $bioH_2$ production in dark and PF mode by studying the responsible genes and carbon metabolism with the help of metabolic engineering. Also, knowledge of distribution of carbon during dark or PF of CW will help to direct the metabolic pathway of $bioH_2$ production toward maximum yield/production rate by directing the flow of energy toward reducing equivalent NADPH, which ultimately leads to $bioH_2$ production. Further, a geothermal energy–based system could be developed to promote economic $bioH_2$ production in coming time, whose energy can be utilized efficiently for maintaining required reaction temperature during CW-dependent DF by using extremophiles.

Lactate production from CW and fermentative conversion of lactose/lactic acid/organic acids present in CW to $bioH_2$ via PF or by two-stage fermentation can be made more feasible by the following measures:

(i) Single-stage PF with the participation of PNS bacteria under optimum pH and temperature, using the lactic acid present in CW for $bioH_2$ production. *R. sphaeroides* O.U.001 was used at a light intensity of 9 Klux and 7 pH to produce 3.6 L of H_2 L^{-1} at a substrate concentration of 40% v/v [83].

(ii) Capnophilic lactic fermentation (CLF) has been considered to be an alternative of DF and is known to produce more $bioH_2$ by degrading carbohydrates containing substrates as compared to DF [84]. CLF is based on integrated glucose with second-stage PF of spent media by using cells of *Thermotoga neapolitana* DSM4359 for CLF and *R. palustris* for PF, respectively. PNS bacteria in subsequent PF utilized the lactic acid present in the spent media of *T. neapolitana,* giving a major yield of $bioH_2$. The combined fermentation system gave an enhanced $bioH_2$ yield of 9.4 ± 1.0 mol mol^{-1} glucose as compared to a yield of 2.6 ± 0.1 mol mol^{-1} glucose by capnophilic fermentation and 6.8 ± 0.9 mol mol^{-1} glucose by PF [84]. In another study, a sequential lactic-photo fermentation approach was done to ferment bread waste by *L. amylovorus* DSM 20532 at 37°C and 85 rpm. The organic acid so produced by this strain was further utilized by *R. palustris* 42OL for second-stage PF at a temperature of 25–28°C and a light intensity of 40 W m^{-2}, giving a maximum $bioH_2$ yield of 3.1 mol mol^{-1} glucose [85].

Some of the checkpoints for utilizing CW for PF are as follows: (i) presence of any H_2-consuming bacteria in $bioH_2$ production media; (ii) less light penetration inside the photobioreactor in case of opaque-colored fermentation broth; (iii) pretreatment of organic

Table 8 Findings involving the use of CFD simulation in bioH_2 production system

Reactor type	Spatial dimensions	Phase model	Numeric method used	Fluid property	CFD model	CFD code	Outcome	Refs
CSTR (17 L)	3-D	Gas-liquid two-phase	MRF	Newtonian	Euler-Euler	ANSYS-CFX	Hydrodynamics characteristics/gas-liquid flow pattern of CSTR-based bioH_2 production system was studied, optimized impeller design by using a CFD model	[126]
CSTR (17 L)	2-D	Gas-liquid two-phase	-	Newtonian	Euler-Euler	ANSYS-CFX	Optimized reactor, based on optimum impeller speed and its diameter Stagnation zone and velocity heterogeneity were found to be important for optimization in CSTR	[77]
CSTR	3-D	RANS in single-phase and Euler-Euler in two-phase	MRF	Newtonian	RANS and Euler-Euler	Fluent 6.3	Operational features and two-phase flow hydrodynamics behavior of stirred tank reactor having vortex ingesting dual impeller were studied by CFD model	[127]
Batch (1 L)	3-D	Gas-liquid two-phase	-	Newtonian	-	ANSYS-CFX	CFD-based simulation confirms uniform temperature distribution and fermentation media velocity inside the annular PBR toward turbulent flow	[72]
CSTR (25L)	3-D	Gas-liquid two-phase	MRF	Newtonian	-	Fluent 14.5	CFD-based simulation predicted PB4 type of impeller to be optimum, which leads to the highest H_2 productivity	[78]
CSTR (36 L)	3-D	Three-phase	MRF	Newtonian	Euler-Euler	Fluent 14.5	Flow pattern and three-phase separator were studied to optimize agitation speed in HCSTR	[80]
STR	2-D	Liquid phase and gas phase	-	Non-newtonian	k-ε turbulence	Fluent 14.0	CFD model was employed to investigate mixing mode and power consumption in anaerobic mono- and codigestion	[128]
Tubular b	2-D	Gas and liquid phase	-	Newtonian	Volume element model	Fluent	Mathematical and computational modeling method helped in studying heat transfer inside the photobioreactor and were suitable for increasing the performance of PFHP	[82]
CSTR (0.23 L)	2-D	Liquid and gas phase	MRF	Newtonian	-	ANSYS Fluent 17.0	CFD analysis helped in predicting interactions among various relevant variables and allowed analysis of rate of reaction along with H_2 flux	[74]

RTD residence time distribution, *RANS* Reynolds-averaged Navier-Stokes, *MRF* moving reference frame, *STR* stirred tank reactor, *PFHP* photofermentative hydrogen production

acids to kill any contaminant, which may decrease the bioH_2 yield; and (iv) filtration to avoid any colloidal particles present in CW. Solving these problems is the need of the hour for a sustainable bioH_2 production system, which will directly lead to the practical implementation of single-stage PF leading to a higher yield of bioH_2.

Engineering research is required for improving bioH_2 production, (i) inhibiting production of by-products such as propionic acid, alcohol, and lactic acid either by genetic engineering approach or by changing HRT/temperature in case of continuous DF system, (ii) developing thermophilic bacterial strain that can directly utilize the lignocellulosic biomass for the cost-effective bioH_2 generation, (iii) using suitable mathematical models to study kinetics of substrate utilization during DF from CW, (v) selecting suitable bioreactor design with appropriate height-to-diameter ratio, (vi) improving the resistance power of photofermentative bacteria against stress conditions, (vii) applying CFD simulation to maintain the optimum temperature inside the PBR and to study the nature of fermentation broth inside the PBR [72], (viii) using certain mathematical optimization tools (FFD, BBD, and CCD) to predict the interaction effects of multiple bioprocess variables on photofermentative bioH_2 production, and (ix) utilizing different sources of light along with optimum light intensity for PF to convert lactic acid into more bioH_2 [85].

Answering of the abovementioned hurdles in the future will lead to the development of a closed-loop and sustainable bioH_2 production system, which will convert CW by utilizing the fermentative waste of one process as feedstock for another process, and will produce renewable, cheaper, and clean H_2 energy.

Acknowledgements The authors wish to express their gratitude to the economic support and facility received from Dr. B. R. Ambedkar National Institute of Technology, Jalandhar (India).

Author contribution First author, Raman Rao, had the idea of writing this review article, and he performed the literature survey and data research. This is later critically revised by corresponding author Dr. Nitai Basak.

Funding No specific grant was received.

Declarations

Research involving human participants and/or animals Not applicable.

Consent to participate Not applicable.

Competing interests The authors declare no competing interests.

References

1. Dutta, S. (2014). A review on production, storage of hydrogen and its utilization as an energy resource. *Journal of Industrial and Engineering Chemistry, 20*, 1148–1156.
2. Osman, A. I., Hefny, M., Maksoud, M. A., Elgarahy, A. M., & Rooney, D. W. (2020). Recent advances in carbon capture storage and utilisation technologies: a review. *Environmental Chemistry Letters*, 1–53.
3. Osman, A. I., Deka, T. J., Baruah, D. C., & Rooney, D. W. (2020). Critical challenges in biohydrogen production processes from the organic feedstocks. *Biomass Conversion and Biorefinery*, 1–19.

4. Phanduang, O., Lunprom, S., Salakkam, A., Liao, Q., & Reungsang, A. (2019). Improvement in energy recovery from Chlorella sp. biomass by integrated dark-photo biohydrogen production and dark fermentation-anaerobic digestion processes. *International Journal of Hydrogen Energy, 44*, 23899–23911.
5. Banu, J. R., Kavitha, S., Kannah, R. Y., Bhosale, R. R., & Kumar, G. (2020). Industrial wastewater to biohydrogen: possibilities towards successful biorefinery route. *Bioresource Technology, 298*, 122378.
6. Zhang, Q., Zhang, Z., Wang, Y., Lee, D.-J., Li, G., Zhou, X., Jiang, D., Xu, B., Lu, C., & Li, Y. (2018). Sequential dark and photo fermentation hydrogen production from hydrolyzed corn stover: a pilot test using 11 m^3 reactor. *Bioresource Technology, 253*, 382–386.
7. Mishra, P., Krishnan, S., Rana, S., Singh, L., Sakinah, M., & Ab Wahid, Z. (2019). Outlook of fermentative hydrogen production techniques: an overview of dark, photo and integrated dark-photo fermentative approach to biomass. *Energy Strategy Reviews, 24*, 27–37.
8. Soares, J. F., Confortin, T. C., Todero, I., Mayer, F. D., & Mazutti, M. A. (2020). Dark fermentative biohydrogen production from lignocellulosic biomass: technological challenges and future prospects. *Renewable and Sustainable Energy Reviews, 117*, 109484.
9. Castelló, E., Ferraz-Junior, A. D. N., Andreani, C., del Pilar Anzola-Rojas, M., Borzacconi, L., Buitrón, G., Carrillo-Reyes, J., Gomes, S. D., Maintinguer, S. I., & Moreno-Andrade, I. (2020). Stability problems in the hydrogen production by dark fermentation: possible causes and solutions. *Renewable and Sustainable Energy Reviews, 119*, 109602.
10. Ghimire, A., Frunzo, L., Pirozzi, F., Trably, E., Escudie, R., Lens, P. N., & Esposito, G. (2015). A review on dark fermentative biohydrogen production from organic biomass: process parameters and use of by-products. *Applied Energy, 144*, 73–95.
11. Swartz, J. (2020). Opportunities toward hydrogen production biotechnologies. *Current Opinion in Biotechnology, 62*, 248–255.
12. Akhlaghi, N., & Najafpour-Darzi, G. (2020). A comprehensive review on biological hydrogen production. *International Journal of Hydrogen Energy*.
13. Vasconcelos, E., Leitão, R., & Santaella, S. (2016). Factors that affect bacterial ecology in hydrogen-producing anaerobic reactors. *Bioenergy Research, 9*, 1260–1271.
14. Hitam, C., & Jalil, A. (2020). A review on biohydrogen production through photo-fermentation of lignocellulosic biomass. *Biomass Conversion and Biorefinery*, 1–19.
15. Sybounya, S., & Nitisoravut, R. (2020). Hybrid composite of modified commercial activated carbon and Zn-Ni hydrotalcite for fermentative hydrogen production. *Journal of Environmental Chemical Engineering, 9*, 104801.
16. Basak, N., Jana, A. K., & Das, D. (2014). Optimization of molecular hydrogen production by *Rhodobacter sphaeroides* OU 001 in the annular photobioreactor using response surface methodology. *International Journal of Hydrogen Energy, 39*, 11889–11901.
17. Basak, N., Jana, A. K., Das, D., & Saikia, D. (2014). Photofermentative molecular biohydrogen production by purple-non-sulfur (PNS) bacteria in various modes: the present progress and future perspective. *International Journal of Hydrogen Energy, 39*, 6853–6871.
18. Canbay, E., Kose, A., & Oncel, S. S. (2018). Photobiological hydrogen production via immobilization: understanding the nature of the immobilization and investigation on various conventional photobioreactors. *3 Biotech, 8*, 244.
19. Basak, N. Das. *D.*
20. Asunis, F., De Gioannis, G., Dessì, P., Isipato, M., Lens, P. N., Muntoni, A., Polettini, A., Pomi, R., Rossi, A., & Spiga, D. (2020). The dairy biorefinery: integrating treatment processes for cheese whey valorisation. *Journal of Environmental Management, 276*, 111240.
21. Prabakar, D., Manimudi, V. T., Sampath, S., Mahapatra, D. M., Rajendran, K., & Pugazhendhi, A. (2018). Advanced biohydrogen production using pretreated industrial waste: outlook and prospects. *Renewable and Sustainable Energy Reviews, 96*, 306–324.
22. Navarro, R., Sanchez-Sanchez, M., Alvarez-Galvan, M., Del Valle, F., & Fierro, J. (2009). Hydrogen production from renewable sources: biomass and photocatalytic opportunities. *Energy & Environmental Science, 2*, 35–54.
23. Azbar, N., & Dokgoz, F. T. C. (2010). The effect of dilution and L-malic acid addition on bio-hydrogen production with *Rhodopseudomonas palustris* from effluent of an acidogenic anaerobic reactor. *International Journal of Hydrogen Energy, 35*, 5028–5033.
24. Prazeres, A. R., Carvalho, F., & Rivas, J. (2012). Cheese whey management: a review. *Journal of Environmental Management, 110*, 48–68.
25. Montecchio, D., Yuan, Y., & Malpei, F. (2018). Hydrogen production dynamic during cheese whey dark fermentation: new insights from modelization. *International Journal of Hydrogen Energy, 43*, 17588–17601.

26. Westermann, P., Jørgensen, B., Lange, L., Ahring, B. K., & Christensen, C. H. (2007). Maximizing renewable hydrogen production from biomass in a bio/catalytic refinery. *International Journal of Hydrogen Energy, 32*, 4135–4141.
27. Argun, H., & Kargi, F. (2011). Bio-hydrogen production by different operational modes of dark and photo-fermentation: an overview. *International Journal of Hydrogen Energy, 36*, 7443–7459.
28. Zhang, Z., Li, Y., Zhang, H., He, C., & Zhang, Q. (2017). Potential use and the energy conversion efficiency analysis of fermentation effluents from photo and dark fermentative bio-hydrogen production. *Bioresource Technology, 245*, 884–889.
29. Zhang, L., Wang, Y.-Z., Zhao, T., & Xu, T. (2019). Hydrogen production from simultaneous saccharification and fermentation of lignocellulosic materials in a dual-chamber microbial electrolysis cell. *International Journal of Hydrogen Energy, 44*, 30024–30030.
30. Sathyaprakasan, P., & Kannan, G. (2015). Economics of bio-hydrogen production. *International Journal of Environmental Science and Development, 6*, 352.
31. Karthic, P., & Joseph, S. (2012). Comparison and limitations of biohydrogen production processes. *Research of Journal Biotechnology, 7*, 59–71.
32. Sarma, S. J., Brar, S. K., Le Bihan, Y., & Buelna, G. (2013). Liquid waste from bio-hydrogen production–a commercially attractive alternative for phosphate solubilizing bio-fertilizer. *International Journal of Hydrogen Energy, 38*, 8704–8707.
33. Chen, W., Chen, S., Chao, S., & Jian, Z. (2011). Butanol production from the effluent of hydrogen fermentation. *Water Science and Technology, 63*, 1236–1240.
34. Reddy, M. V., Amulya, K., Rohit, M., Sarma, P., & Mohan, S. V. (2014). Valorization of fatty acid waste for bioplastics production using *Bacillus tequilensis*: integration with dark-fermentative hydrogen production process. *International Journal of Hydrogen Energy, 39*, 7616–7626.
35. Devi, M. P., Subhash, G. V., & Mohan, S. V. (2012). Heterotrophic cultivation of mixed microalgae for lipid accumulation and wastewater treatment during sequential growth and starvation phases: effect of nutrient supplementation. *Renewable Energy, 43*, 276–283.
36. Macwan, S. R., Dabhi, B. K., Parmar, S., & Aparnathi, K. (2016). Whey and its utilization. *International Journal of Current Microbiology and Applied Sciences, 5*, 134–155.
37. Farizoglu, B., Keskinler, B., Yildiz, E., & Nuhoglu, A. (2004). Cheese whey treatment performance of an aerobic jet loop membrane bioreactor. *Process Biochemistry, 39*, 2283–2291.
38. Siso, M. G. (1996). The biotechnological utilization of cheese whey: a review. *Bioresource Technology, 57*, 1–11.
39. Azbar, N., Dokgöz, F. T. Ç., & Peker, Z. (2009). Optimization of basal medium for fermentative hydrogen production from cheese whey wastewater. *International Journal of Green Energy, 6*, 371–380.
40. Lappa, I. K., Papadaki, A., Kachrimanidou, V., Terpou, A., Koulougliotis, D., Eriotou, E., & Kopsahelis, N. (2019). Cheese whey processing: integrated biorefinery concepts and emerging food applications. *Foods, 8*, 347.
41. Escalante, H., Castro, L., Amaya, M., Jaimes, L., & Jaimes-Estévez, J. (2018). Anaerobic digestion of cheese whey: energetic and nutritional potential for the dairy sector in developing countries. *Waste Management, 71*, 711–718.
42. Ahmad, T., Aadil, R. M., Ahmed, H., ur Rahman, U., Soares, B. C., Souza, S. L., Pimentel, T. C., Scudino, H., Guimarães, J. T., & Esmerino, E. A. (2019). Treatment and utilization of dairy industrial waste: a review. *Trends Food Science Technology, 88*, 361–372.
43. Nagarajan, D., Nandini, A., Dong, C.-D., Lee, D.-J., & Chang, J.-S. (2020). Lactic acid production from renewable feedstocks using poly (vinyl alcohol)-immobilized *Lactobacillus plantarum* 23. *Industrial and Engineering Chemistry Research, 59*, 17156–17164.
44. Oshiro, M., Shinto, H., Tashiro, Y., Miwa, N., Sekiguchi, T., Okamoto, M., Ishizaki, A., & Sonomoto, K. (2009). Kinetic modeling and sensitivity analysis of xylose metabolism in *Lactococcus lactis* IO-1. *Journal of Bioscience and Bioengineering, 108*, 376–384.
45. Abdel-Rahman, M. A., Tashiro, Y., & Sonomoto, K. (2011). Lactic acid production from lignocellulose-derived sugars using lactic acid bacteria: overview and limits. *Journal of Biotechnology, 156*, 286–301.
46. Okano, K., Yoshida, S., Tanaka, T., Ogino, C., Fukuda, H., & Kondo, A. (2009). Homo-D-lactic acid fermentation from arabinose by redirection of the phosphoketolase pathway to the pentose phosphate pathway in L-lactate dehydrogenase gene-deficient *Lactobacillus plantarum*. *Applied and Environmental Microbiology, 75*, 5175–5178.
47. Holzapfel, W. H., & Wood, B. J. (2014). *Lactic acid bacteria: biodiversity and taxonomy*. John Wiley & Sons.
48. Sinha, P., Roy, S., & Das, D. (2015). Role of formate hydrogen lyase complex in hydrogen production in facultative anaerobes. *International Journal of Hydrogen Energy, 40*, 8806–8815.

49. Sawers, G. (1994). The hydrogenases and formate dehydrogenases of *Escherichia coli*. *Antonie Van Leeuwenhoek, 66*, 57–88.
50. Bagramyan, K., & Trchounian, A. (2003). Structural and functional features of formate hydrogen lyase, an enzyme of mixed-acid fermentation from *Escherichia coli*. *Biochemistry (Moscow), 68*, 1159–1170.
51. da Silva, A. N., Macêdo, W. V., Sakamoto, I. K., Pereyra, D. d. L. A. D., Mendes, C. O., Maintinguer, S. I., Caffaro Filho, R. A., Damianovic, M. H. Z., Varesche, M. B. A., & de Amorim, E. L. C. (2019). Biohydrogen production from dairy industry wastewater in an anaerobic fluidized-bed reactor. *Biomass and Bioenergy, 120*, 257–264.
52. Romão, B. B., Silva, F. T. M., de Barcelos Costa, H. C., do Carmo, T. S., Cardoso, S. L., de Souza Ferreira, J., Batista, F. R. X., & Cardoso, V. L. (2019). Alternative techniques to improve hydrogen production by dark fermentation. *3 Biotech, 9*, 18.
53. Lima, D., Lazaro, C., Rodrigues, J., Ratusznei, S., & Zaiat, M. (2016). Optimization performance of an AnSBBR applied to biohydrogen production treating whey. *Journal of Environmental Management, 169*, 191–201.
54. Castelló, E., Braga, L., Fuentes, L., & Etchebehere, C. (2018). Possible causes for the instability in the H_2 production from cheese whey in a CSTR. *International Journal of Hydrogen Energy, 43*, 2654–2665.
55. Blanco, V., Oliveira, G., & Zaiat, M. (2019). Dark fermentative biohydrogen production from synthetic cheese whey in an anaerobic structured-bed reactor: performance evaluation and kinetic modeling. *Renewable Energy, 139*, 1310–1319.
56. Sarma, S. J., Pachapur, V., Brar, S. K., Le Bihan, Y., & Buelna, G. (2015). Hydrogen biorefinery: potential utilization of the liquid waste from fermentative hydrogen production. *Renewable and Sustainable Energy Reviews, 50*, 942–951.
57. Silva, F. T. M., Bessa, L. P., Vieira, L. M., Moreira, F. S., de Souza Ferreira, J., Batista, F. R. X., & Cardoso, V. L. (2019). Dark fermentation effluent as substrate for hydrogen production from *Rhodobacter capsulatus* highlighting the performance of different fermentation systems. *3 Biotech, 9*, 153.
58. Rao, R., & Basak, N. (2020). Development of novel strategies for higher fermentative biohydrogen recovery along with novel metabolites from organic wastes: the present state of the art. *Biotechnology and Applied Biochemistry*.
59. Azwar, M., Hussain, M., & Abdul-Wahab, A. (2014). Development of biohydrogen production by photobiological, fermentation and electrochemical processes: a review. *Renewable and Sustainable Energy Reviews, 31*, 158–173.
60. Baeyens, J., Zhang, H., Nie, J., Appels, L., Dewil, R., Ansart, R., & Deng, Y. (2020). Reviewing the potential of bio-hydrogen production by fermentation. *Renewable and Sustainable Energy Reviews, 131*, 110023.
61. Basak, N., & Das, D. (2007). The prospect of purple non-sulfur (PNS) photosynthetic bacteria for hydrogen production: the present state of the art. *World Journal of Microbiology and Biotechnology, 23*, 31–42.
62. Rai, P. K., Singh, S., & Asthana, R. (2012). Biohydrogen production from cheese whey wastewater in a two-step anaerobic process. *Applied Biochemistry and Biotechnology, 167*, 1540–1549.
63. Kim, D.-H., & Kim, M.-S. (2013). Development of a novel three-stage fermentation system converting food waste to hydrogen and methane. *Bioresource Technology, 127*, 267–274.
64. Yin, Y., & Wang, J. (2019). Optimization of fermentative hydrogen production by Enterococcus faecium INET2 using response surface methodology. *International Journal of Hydrogen Energy, 44*, 1483–1491.
65. Lopez-Hidalgo, A. M., Alvarado-Cuevas, Z. D., & De Leon-Rodriguez, A. (2018). Biohydrogen production from mixtures of agro-industrial wastes: chemometric analysis, optimization and scaling up. *Energy, 159*, 32–41.
66. Mishra, P., Singh, L., Ab Wahid, Z., Krishnan, S., Rana, S., Islam, M. A., Sakinah, M., Ameen, F., & Syed, A. (2018). Photohydrogen production from dark-fermented palm oil mill effluent (DPOME) and statistical optimization: renewable substrate for hydrogen. *Journal of Cleaner Production, 199*, 11–17.
67. Rao, R., & Basak, N. (2020). Optimization and modelling of dark fermentative hydrogen production from cheese whey by Enterobacter aerogenes 2822. *International Journal of Hydrogen Energy, 46*, 1777–1800.
68. Zainal, B. S., Zinatizadeh, A. A., Chyuan, O. H., Mohd, N. S., & Ibrahim, S. (2018). Effects of process, operational and environmental variables on biohydrogen production using palm oil mill effluent (POME). *International Journal of Hydrogen Energy, 43*, 10637–10644.
69. Sagır, E., Yucel, M., & Hallenbeck, P. C. (2018). Demonstration and optimization of sequential microaerobic dark-and photo-fermentation biohydrogen production by immobilized *Rhodobacter capsulatus* JP91. *Bioresource Technology, 250*, 43–52.
70. Mahata, C., Ray, S., & Das, D. (2020). Optimization of dark fermentative hydrogen production from organic wastes using acidogenic mixed consortia. *Energy Conversion and Management, 219*, 113047.

71. Al-Mohammedawi, H. H., Znad, H., & Eroglu, E. (2018). Synergistic effects and optimization of photo-fermentative hydrogen production of *Rhodobacter sphaeroides* DSM 158. *International Journal of Hydrogen Energy*.
72. Basak, N., Jana, A. K., & Das, D. (2016). CFD modeling of hydrodynamics and optimization of photofermentative hydrogen production by *Rhodopseudomonas palustris* DSM 123 in annular photobioreactor. *International Journal of Hydrogen Energy, 41*, 7301–7317.
73. Chezeau, B., & Vial, C. (2019). *Modeling and simulation of the biohydrogen production processes* (pp. 445–483). Amsterdam: Elsevier.
74. Maluta, F., Paglianti, A., & Montante, G. (2019). Modelling of biohydrogen production in stirred fermenters by computational fluid dynamics. *Process Safety and Environment Protection, 125*, 342–357.
75. Brindhadevi, K., Shanmuganathan, R., Pugazhendhi, A., Gunasekar, P., & Manigandan, S. (2020). Biohydrogen production using horizontal and vertical continuous stirred tank reactor-a numerical optimization. *International Journal of Hydrogen Energy*.
76. Wang, J., Xue, Q., Guo, T., Mei, Z., Long, E., Wen, Q., Huang, W., Luo, T., & Huang, R. (2018). A review on CFD simulating method for biogas fermentation material fluid. *Renewable and Sustainable Energy Reviews, 97*, 64–73.
77. Wang, X., Ding, J., Guo, W.-Q., & Ren, N.-Q. (2010). Scale-up and optimization of biohydrogen production reactor from laboratory-scale to industrial-scale on the basis of computational fluid dynamics simulation. *International Journal of Hydrogen Energy, 35*, 10960–10966.
78. Niño-Navarro, C., Chairez, I., Torres-Bustillos, L., Ramírez-Muñoz, J., Salgado-Manjarrez, E., & Garcia-Peña, E. (2016). Effects of fluid dynamics on enhanced biohydrogen production in a pilot stirred tank reactor: CFD simulation and experimental studies. *International Journal of Hydrogen Energy, 41*, 14630–14640.
79. Pan, H., fan Hu, Y., hong Pu, W., fen Dan, J., & kuan Yang, J. (2017). CFD optimization of the baffle angle of an expanded granular sludge bed reactor. *Journal of Environmental Chemical Engineering, 5*, 4531–4538.
80. Ri, P.-C., Ren, N.-Q., Ding, J., Kim, J.-S., & Guo, W.-Q. (2017). CFD optimization of horizontal continuous stirred-tank (HCSTR) reactor for bio-hydrogen production. *International Journal of Hydrogen Energy, 42*, 9630–9640.
81. Zhang, Z., Wu, Q., Zhang, C., Wang, Y., Li, Y., & Zhang, Q. (2014). Effect of inlet velocity on heat transfer process in a novel photo-fermentation biohydrogen production bioreactor using computational fluid dynamics simulation. *Bioresources, 10*, 469–481.
82. Zhiping, Z., Quanguo, Z., Jianzhi, Y., Lianhao, L., Tian, Z., & Zhengbai, L. (2017). CFD modeling and experiment of heat transfer in a tubular photo-bioreactor for photo-fermentation bio-hydrogen production. *International Journal of Agriculture Biology Engineering, 10*, 209–217.
83. Seifert, K., Waligorska, M., & Laniecki, M. (2010). Hydrogen generation in photobiological process from dairy wastewater. *International Journal of Hydrogen Energy, 35*, 9624–9629.
84. Dipasquale, L., Adessi, A., d'Ippolito, G., Rossi, F., Fontana, A., & De Philippis, R. (2015). Introducing capnophilic lactic fermentation in a combined dark-photo fermentation process: a route to unparalleled H_2 yields. *Applied Microbiology and Biotechnology, 99*, 1001–1010.
85. Adessi, A., Venturi, M., Candeliere, F., Galli, V., Granchi, L., & De Philippis, R. (2018). Bread wastes to energy: sequential lactic and photo-fermentation for hydrogen production. *International Journal of Hydrogen Energy, 43*, 9569–9576.
86. Davila-Vazquez, G., Alatriste-Mondragón, F., de León-Rodríguez, A., & Razo-Flores, E. (2008). Fermentative hydrogen production in batch experiments using lactose, cheese whey and glucose: influence of initial substrate concentration and pH. *International Journal of Hydrogen Energy, 33*, 4989–4997.
87. Rosales-Colunga, L. M., Razo-Flores, E., Ordoñez, L. G., Alatriste-Mondragón, F., & De León-Rodríguez, A. (2010). Hydrogen production by *Escherichia coli* ΔhycA ΔlacI using cheese whey as substrate. *International Journal of Hydrogen Energy, 35*, 491–499.
88. Davila-Vazquez, G., de León-Rodríguez, A., Alatriste-Mondragón, F., & Razo-Flores, E. (2011). The buffer composition impacts the hydrogen production and the microbial community composition in non-axenic cultures. *Biomass and Bioenergy, 35*, 3174–3181.
89. Kargi, F., Eren, N. S., & Ozmihci, S. (2012). Bio-hydrogen production from cheese whey powder (CWP) solution: comparison of thermophilic and mesophilic dark fermentations. *International Journal of Hydrogen Energy, 37*, 8338–8342.
90. De Gioannis, G., Friargiu, M., Massi, E., Muntoni, A., Polettini, A., Pomi, R., & Spiga, D. (2014). Biohydrogen production from dark fermentation of cheese whey: influence of pH. *International Journal of Hydrogen Energy, 39*, 20930–20941.

91. Gadhe, A., Sonawane, S. S., & Varma, M. N. (2015). Enhanced biohydrogen production from dark fermentation of complex dairy wastewater by sonolysis. *International Journal of Hydrogen Energy, 40*, 9942–9951.
92. Moreno, R., Escapa, A., Cara, J., Carracedo, B., & Gómez, X. (2015). A two-stage process for hydrogen production from cheese whey: integration of dark fermentation and biocatalyzed electrolysis. *International Journal of Hydrogen Energy, 40*, 168–175.
93. Patel, A. K., Vaisnav, N., Mathur, A., Gupta, R., & Tuli, D. K. (2016). Whey waste as potential feedstock for biohydrogen production. *Renewable Energy, 98*, 221–225.
94. Moreira, F., Machado, R., Romão, B., Batista, F., Ferreira, J., & Cardoso, V. (2017). Improvement of hydrogen production by biological route using repeated batch cycles. *Process Biochemistry, 58*, 60–68.
95. Gokfiliz-Yildiz, P., & Karapinar, I. (2018). Optimization of particle number, substrate concentration and temperature of batch immobilized reactor system for biohydrogen production by dark fermentation. *International Journal of Hydrogen Energy, 43*, 10655–10665.
96. Pandey, A., Srivastava, S., Rai, P., & Duke, M. (2019). Cheese whey to biohydrogen and useful organic acids: a non-pathogenic microbial treatment by *L. acidophilus*. *Scientific Reports, 9*, 1–9.
97. Alvarez-Guzmán, C. L., Cisneros-de la Cueva, S., Balderas-Hernández, V. E., Smoliński, A., & De León-Rodríguez, A. (2020). Biohydrogen production from cheese whey powder by *Enterobacter asburiae:* effect of operating conditions on hydrogen yield and chemometric study of the fermentative metabolites. *Energy Reports, 6*, 1170–1180.
98. Carrillo-Reyes, J., Celis, L. B., Alatriste-Mondragón, F., & Razo-Flores, E. (2012). Different start-up strategies to enhance biohydrogen production from cheese whey in UASB reactors. *International Journal of Hydrogen Energy, 37*, 5591–5601.
99. Perna, V., Castelló, E., Wenzel, J., Zampol, C., Lima, D. F., Borzacconi, L., Varesche, M., Zaiat, M., & Etchebehere, C. (2013). Hydrogen production in an upflow anaerobic packed bed reactor used to treat cheese whey. *International Journal of Hydrogen Energy, 38*, 54–62.
100. Rosa, P. R. F., Santos, S. C., & Silva, E. L. (2014). Different ratios of carbon sources in the fermentation of cheese whey and glucose as substrates for hydrogen and ethanol production in continuous reactors. *International Journal of Hydrogen Energy, 39*, 1288–1296.
101. Rosa, P. R. F., Santos, S. C., Sakamoto, I. K., Varesche, M. B. A., & Silva, E. L. (2014). Hydrogen production from cheese whey with ethanol-type fermentation: effect of hydraulic retention time on the microbial community composition. *Bioresource Technology, 161*, 10–19.
102. Fernández, C., Cuetos, M., Martínez, E., & Gómez, X. (2015). Thermophilic anaerobic digestion of cheese whey: Coupling H_2 and CH_4 production. *Biomass and Bioenergy, 81*, 55–62.
103. Ottaviano, L. M., Ramos, L. R., Botta, L. S., Varesche, M. B. A., & Silva, E. L. (2017). Continuous thermophilic hydrogen production from cheese whey powder solution in an anaerobic fluidized bed reactor: effect of hydraulic retention time and initial substrate concentration. *International Journal of Hydrogen Energy, 42*, 4848–4860.
104. Ghimire, A., Luongo, V., Frunzo, L., Pirozzi, F., Lens, P. N., & Esposito, G. (2017). Continuous biohydrogen production by thermophilic dark fermentation of cheese whey: use of buffalo manure as buffering agent. *International Journal of Hydrogen Energy, 42*, 4861–4869.
105. Argun, H., & Kargi, F. (2010). Photo-fermentative hydrogen gas production from dark fermentation effluent of ground wheat solution: effects of light source and light intensity. *International Journal of Hydrogen Energy, 35*, 1595–1603.
106. Lo, Y.-C., Chen, C.-Y., Lee, C.-M., & Chang, J.-S. (2010). Sequential dark–photo fermentation and autotrophic microalgal growth for high-yield and CO_2-free biohydrogen production. *International Journal of Hydrogen Energy, 35*, 10944–10953.
107. Cheng, J., Su, H., Zhou, J., Song, W., & Cen, K. (2011). Hydrogen production by mixed bacteria through dark and photo fermentation. *International Journal of Hydrogen Energy, 36*, 450–457.
108. Laurinavichene, T. V., Belokopytov, B. F., Laurinavichius, K. S., Khusnutdinova, A. N., Seibert, M., & Tsygankov, A. A. (2012). Towards the integration of dark-and photo-fermentative waste treatment. 4. Repeated batch sequential dark-and photofermentation using starch as substrate. *International Journal of Hydrogen Energy, 37*, 8800–8810.
109. Cheng, J., Xia, A., Liu, Y., Lin, R., Zhou, J., & Cen, K. (2012). Combination of dark-and photo-fermentation to improve hydrogen production from Arthrospira platensis wet biomass with ammonium removal by zeolite. *International Journal of Hydrogen Energy, 37*, 13330–13337.
110. Chookaew, T., Sompong, O., & Prasertsan, P. (2015). Biohydrogen production from crude glycerol by two stage of dark and photo fermentation. *International Journal of Hydrogen Energy, 40*, 7433–7438.
111. Nasr, M., Tawfik, A., Ookawara, S., Suzuki, M., Kumari, S., & Bux, F. (2015). Continuous biohydrogen production from starch wastewater via sequential dark-photo fermentation with emphasize on maghemite nanoparticles. *Journal of Industrial and Engineering Chemistry, 21*, 500–506.

112. Lin, R., Cheng, J., Yang, Z., Ding, L., Zhang, J., Zhou, J., & Cen, K. (2016). Enhanced energy recovery from cassava ethanol wastewater through sequential dark hydrogen, photo hydrogen and methane fermentation combined with ammonium removal. *Bioresource Technology, 214*, 686–691.
113. Mishra, P., Thakur, S., Singh, L., Ab Wahid, Z., & Sakinah, M. (2016). Enhanced hydrogen production from palm oil mill effluent using two stage sequential dark and photo fermentation. *International Journal of Hydrogen Energy, 41*, 18431–18440.
114. Hitit, Z. Y., Lazaro, C. Z., & Hallenbeck, P. C. (2017). Increased hydrogen yield and COD removal from starch/glucose based medium by sequential dark and photo-fermentation using *Clostridium butyricum* and *Rhodopseudomonas palustris*. *International Journal of Hydrogen Energy, 42*, 18832–18843.
115. Cai, J., Zhao, Y., Fan, J., Li, F., Feng, C., Guan, Y., Wang, R., & Tang, N. (2019). Photosynthetic bacteria improved hydrogen yield of combined dark-and photo-fermentation. *Journal of Biotechnology, 302*, 18–25.
116. Dinesh, G. H., Nguyen, D. D., Ravindran, B., Chang, S. W., Vo, D.-V. N., Bach, Q.-V., Tran, H. N., Basu, M. J., Mohanrasu, K., Murugan, R. S., Swetha, T. A., Sivapraksh, G., Selvaraj, A., & Arun, A. (2020). Simultaneous biohydrogen (H2) and bioplastic (poly-β-hydroxybutyrate-PHB) productions under dark, photo, and subsequent dark and photo fermentation utilizing various wastes. *International Journal of Hydrogen Energy, 45*, 5840–5853.
117. Dolly, S., Pandey, A., Pandey, B. K., & Gopal, R. (2015). Process parameter optimization and enhancement of photo-biohydrogen production by mixed culture of *Rhodobacter sphaeroides* NMBL-02 and *Escherichia coli* NMBL-04 using Fe-nanoparticle. *International Journal of Hydrogen Energy, 40*, 16010–16020.
118. Sangyoka, S., Reungsang, A., & Lin, C.-Y. (2016). Optimization of biohydrogen production from sugarcane bagasse by mixed cultures using a statistical method. *Sustainable Environment Resources, 26*, 235–242.
119. de Oliveira Faber, M., & Ferreira-Leitão, V. S. (2016). Optimization of biohydrogen yield produced by bacterial consortia using residual glycerin from biodiesel production. *Bioresour. Technol., 219*, 365–370.
120. Akhlaghi, M., Boni, M. R., De Gioannis, G., Muntoni, A., Polettini, A., Pomi, R., Rossi, A., & Spiga, D. (2017). A parametric response surface study of fermentative hydrogen production from cheese whey. *Bioresource Technology, 244*, 473–483.
121. Asadi, N., & Zilouei, H. (2017). Optimization of organosolv pretreatment of rice straw for enhanced biohydrogen production using *Enterobacter aerogenes*. *Bioresource Technology, 227*, 335–344.
122. Sewsynker-Sukai, Y., & Kana, E. B. G. (2017). Does the volume matter in bioprocess model development? An insight into modelling and optimization of biohydrogen production. *International Journal of Hydrogen Energy, 42*, 5780–5792.
123. Lopez-Hidalgo, A. M., Alvarado-Cuevas, Z. D., & De León-Rodríguez, A. (2018). Biohydrogen production from mixtures of agro-industrial wastes: chemometric analysis, optimization and scaling up. *Energy.*
124. Ulhiza, T. A., Puad, N. I. M., & Azmi, A. S. (2018). Optimization of culture conditions for biohydrogen production from sago wastewater by *Enterobacter aerogenes* using response surface methodology. *International Journal of Hydrogen Energy, 43*, 22148–22158.
125. de la Cueva, S. C., Guzmán, C. L. A., Hernández, V. E. B., & Rodríguez, A. D. L. (2018). Optimization of biohydrogen production by the novel psychrophilic strain N92 collected from the Antarctica. *International Journal of Hydrogen Energy, 43*, 13798–13809.
126. Ding, J., Wang, X., Zhou, X.-F., Ren, N.-Q., & Guo, W.-Q. (2010). CFD optimization of continuous stirred-tank (CSTR) reactor for biohydrogen production. *Bioresource Technology, 101*, 7005–7013.
127. Montantea, G., Coroneoa, M., Francesconib, J., Pagliantia, A., & Magellia, F. (2012). CFD modelling of a novel stirred reactor for the bio-production of hydrogen. *Simulation, 10*, 12.
128. Zhang, Y., Yu, G., Yu, L., Siddhu, M. A., Gao, M., Abdeltawab, A. A., Al-Deyab, S. S., & Chen, X. (2016). Computational fluid dynamics study on mixing mode and power consumption in anaerobic mono- and co-digestion. *Bioresource Technology, 203*, 166–172.